

# IOWA STATE UNIVERSITY

## Department of Economics

---

### Economics Working Papers

---

12-23-2019

Working Paper Number 19014

## A Test System for ERCOT Market Design Studies: Development and Application

Swathi Battula

*Iowa State University*, [swathi@iastate.edu](mailto:swathi@iastate.edu)

Leigh Tesfatsion

*Iowa State University*, [tesfatsi@iastate.edu](mailto:tesfatsi@iastate.edu)

Thomas E. McDermott

*Pacific Northwest National Laboratory*

Original Release Date: September 11, 2019

Revision: September 19, 2019

Latest Revision: December 23, 2019

Follow this and additional works at: [https://lib.dr.iastate.edu/econ\\_workingpapers](https://lib.dr.iastate.edu/econ_workingpapers)



Part of the [Industrial Organization Commons](#), [Oil, Gas, and Energy Commons](#), and the [Power and Energy Commons](#)

---

### Recommended Citation

Battula, Swathi; Tesfatsion, Leigh; and McDermott, Thomas E., "A Test System for ERCOT Market Design Studies: Development and Application" (2019). *Economics Working Papers*: Department of Economics, Iowa State University. 19014.

[https://lib.dr.iastate.edu/econ\\_workingpapers/79](https://lib.dr.iastate.edu/econ_workingpapers/79)

Iowa State University does not discriminate on the basis of race, color, age, ethnicity, religion, national origin, pregnancy, sexual orientation, gender identity, genetic information, sex, marital status, disability, or status as a U.S. veteran. Inquiries regarding non-discrimination policies may be directed to Office of Equal Opportunity, 3350 Beardshear Hall, 515 Morrill Road, Ames, Iowa 50011, Tel. 515 294-7612, Hotline: 515-294-1222, email [eooffice@mail.iastate.edu](mailto:eooffice@mail.iastate.edu).

This Working Paper is brought to you for free and open access by the Iowa State University Digital Repository. For more information, please visit [lib.dr.iastate.edu](https://lib.dr.iastate.edu).

---

# A Test System for ERCOT Market Design Studies: Development and Application

## Abstract

The ERCOT Test System developed in this study is an open-source library of Java/Python software classes, together with a synthetic grid construction method, specifically designed to facilitate the study of ERCOT market operations over successive days. In default form, these classes permit a high-level modeling of existing ERCOT market operations. Users can conduct a broad range of computational experiments under alternative parameter settings. In addition, users can readily extend these classes to model additional existing or envisioned ERCOT market features to suit different research purposes. An 8-bus test case is used to illustrate the capabilities of the test system. Ongoing studies making use of the test system to model larger-scale transmission components for integrated transmission and distribution systems are also reported.

## Keywords

Test system, ERCOT, wholesale power market, multi-day market operations, performance evaluation, Java, Python, open source

## Disciplines

Electrical and Computer Engineering | Industrial Organization | Oil, Gas, and Energy | Power and Energy

# A Test System for ERCOT Market Design Studies: Development and Application<sup>☆</sup>

Swathi Battula<sup>a</sup>, Leigh Tesfatsion<sup>b</sup>, Thomas E. McDermott<sup>c</sup>

<sup>a</sup>*Depart. of Electrical & Computer Eng.*, <sup>b</sup>*Depart. of Econ., Iowa State U., Ames, IA 50011, USA*; <sup>c</sup>*Pacific Northwest National Laboratory, Richland, WA 99354.*

---

## Abstract

The ERCOT Test System developed in this study is an open-source library of Java/Python software classes, together with a synthetic grid construction method, specifically designed to facilitate the study of ERCOT market operations over successive days. In default form, these classes permit a high-level modeling of existing ERCOT market operations. Users can conduct a broad range of computational experiments under alternative parameter settings. In addition, users can readily extend these classes to model additional existing or envisioned ERCOT market features to suit different research purposes. An 8-bus test case is used to illustrate the capabilities of the test system. Ongoing studies making use of the test system to model larger-scale transmission components for integrated transmission and distribution systems are also reported.

*Keywords:* Test system, ERCOT, wholesale power market, multi-day market operations, performance evaluation, Java, Python, open source

---

## 1. Introduction

The ERCOT Test System developed in this study is specifically designed to facilitate market studies for the U.S. *Electric Reliability Council of Texas*

---

<sup>☆</sup>This work was supported by contract #339051 with the Pacific Northwest National Laboratory operated for the U.S. DOE under contract DE-AC65-76RLO1830, and by contract DE-OE 0000839 with the U.S. DOE Office of Electricity (OE). Corresponding author: Leigh Tesfatsion (tesfatsi@iastate.edu), Department of Economics, Iowa State University, Heady Hall 260, Ames, IA 50011-1054, USA.

(*ERCOT*) energy region. The test system comprises an open-source library of Java/Python software classes, together with a synthetic grid construction method, permitting the modeling of ERCOT’s ISO-managed wholesale power market operating over a high-voltage transmission grid during successive days with continually updated system conditions.

Table 1: Three Possible Use Levels for the ERCOT Test System

Level	Use Description
Default	High-level user-configured modeling of existing ERCOT market operations over a user-configured transmission grid
Extended	Extended software classes permitting study of additional or newly envisioned ERCOT market design features
Coupled	Activation of high-level architecture flag permitting the test system to be integrated as a component of a coupled system, such as an integrated transmission and distribution system

As indicated in Table 1, the ERCOT Test System can be used at three different levels, depending on the research purpose at hand. In default form, the test system supports a high-level user-configured modeling of existing ERCOT market operations over a user-configured transmission grid. Users can conduct a broad range of computational experiments under alternative parameter settings determining the attributes of market participants and the size and topology of the transmission grid. An 8-bus test case is reported to provide a concrete demonstration of these capabilities.

In addition, users can readily extend the test system’s software classes to model and study additional existing or newly envisioned ERCOT market features. Users can also integrate the test system as a component subsystem of the Framework for Network Co-Simulation (FNCS) [1], a high-level simulation architecture developed at the Pacific Northwest National Laboratory (PNNL), simply by setting a FNCSActive flag to 1. To illustrate this flexibility, Iowa State University (ISU) and PNNL studies making use of the ERCOT Test System to model transmission components for Integrated Transmission and Distribution (ITD) systems are reported.

The organization of this study is as follows. Related literature is reviewed in Section 2. Section 3 provides a brief overview of current ERCOT market operations. The key features of the market component for the ERCOT Test System are described in Section 4. The bus and line construction methods

comprising the grid component of the test system are carefully explained in Section 5. These methods are used in Section 6 to construct a relatively small 8-bus ERCOT test grid suitable for DC optimal power flow and DC power flow analyses for which voltage problems are not an issue.

The resulting grid, referred to as the 8-Bus ERCOT DC Test Grid, is extended in Sections 7–8 to a complete 8-Bus ERCOT test case. This test case illustrates the ability of the ERCOT Test System to model ERCOT day-ahead and real-time markets operating over a transmission grid during successive days with continually updated system operating conditions.

Section 9 discusses how the ERCOT Test System with enabled FNCS is being used to support Transactive Energy System (TES) design studies for ITD systems. The section first briefly describes ongoing ITD TES design work at ISU [2] for which the transmission component is implemented by means of ERCOT test cases with relatively small 8-bus grids. The main focus of this ISU work is on efficiency and welfare implications. The section next describes ongoing ITD TES design work at PNNL [3] for which the transmission component is implemented by means of a 200-bus ERCOT test case. This larger-scale test case is suitable for AC optimal power flow and AC power flow studies with potential for voltage problems. PNNL researchers are using this larger-scale test case to explore the effects of contingency and congestion effects on alternative market mechanisms.

Section 10 concludes. Nomenclature tables and technical implementation details are provided in appendices A through D. Code and data for the ERCOT Test System and test cases can be accessed at [4].

## 2. Related Literature

Previously developed open-source test systems have largely been designed as support tools for the study of power system reliability at relatively small time-scales. In contrast, the ERCOT Test System provides an open-source support tool for the study of ERCOT’s market operations over successive days of operation.

These previously developed systems include the IEEE reliability test systems stored at the University of Washington archive [5, 6] as well as more recently developed test systems such as [7, 8]. For example, ref. [8] conducts a power flow study for a 68-bus system to determine initial steady-state values; and state-space matrices and eigenvalues are then determined for the linearized system at this initial point to verify system constraints are met.

The traditional IEEE test-system focus on power flow problems for reliability analysis has been extended in more recent test systems and software packages to permit a consideration of Optimal Power Flow (OPF) solutions based on the bids and offers of market participants. This development reflects the increasing use of OPF optimizations in centrally-managed wholesale power markets. For example, MATPOWER [9] is a package of Matlab M-files designed for solving both power flow and OPF problems. Nevertheless, the focus of MATPOWER is still on reliability issues arising at relatively small time-scales.

Some previous researchers have attempted to redress the relative lack of publicly available market-oriented test systems. For example, variants of a 5-bus test system originally developed in 2002 by John Lally [10, Section 6] for the study of the financial transmission rights market in ISO-NE are now being used for more general market training by ISO-NE, PJM, and other ISO/RTO-managed U.S. energy regions.

As detailed in [11, 12], the Lally 5-bus test system has been developed into a more fully articulated 5-Bus Test Case included (along with a 2-Bus Test Case and a 30-Bus Test Case) in the V2.06 release of the AMES Wholesale Power Market Test Bed [13]. In addition, Li and Bo [14] have suggested various ways to improve a version of the Lally 5-bus test system in use by PJM, such as the introduction of differentiated loads across the three load buses for increased clarity. Li and Bo also discuss a number of modifications proposed by themselves and others for the IEEE 30-bus reliability test system that would increase its usefulness for market study purposes.

However, the structural attributes for these small-scale market-oriented test systems (e.g., grid configuration, generation and load locations) are pre-set, for illustrative purposes only. Users are not able to experiment with alternative settings for these structural attributes.

Larger-scale market-oriented test systems have also been developed, such as the FERC test system [15] and the WECC test system [16]. The FERC test system provides a large-scale PJM-based data set and unit commitment (UC) formulation to facilitate the comparative study of alternative DAM and residual UC solvers. The 240-bus WECC test system provides a realistic large-scale test system for the California Independent System Operator (CAISO) and the Western Electricity Coordination Council (WECC) for the purpose of studying possible improvements to existing market features.

However, these larger-scale test systems have been designed for commercial-grade application, not for exploratory fast-execution simulation studies. More-

over, they are not open source and hence are not easy to access for most researchers. Finally, the systems are so large and complex that it is difficult for researchers to make use of them even if they are able to gain access.

The closest work to the current study is by Krishnamurthy et al. [17]. The authors develop an 8-zone test system based on ISO-NE data and ISO-NE’s grid configuration. However, the purpose of this 8-zone test system is to permit comparative performance evaluation of stochastic versus deterministic formulations for ISO-NE’s use of security-constrained unit commitment optimizations in its day-ahead market operations. No attempt is made to model ISO-NE market operations more fully. For example, real-time market operations are not modeled.

In contrast, the ERCOT Test System implements ERCOT day-ahead and real-time market processes over successive days of operation by means of AMES V5.0 [18, 19], an open-source platform that models salient common operational features of day-ahead and real-time market operations in U.S. ISO/RTO-managed wholesale power markets operating over high-voltage transmission grids. In addition, building on prior work by Tom Overbye and his collaborators [20]-[26], the ERCOT Test System also permits users to construct empirically-based ERCOT test grids with sizes scaled appropriately for different research purposes.

### 3. ERCOT Wholesale Power Market Operations

#### 3.1. ERCOT Day-Ahead and Real-Time Markets

ERCOT wholesale power market operations are complicated [27, 28, 29, 30]. However, at its core, the ERCOT wholesale power market consists of a *Day-Ahead Market (DAM)* operating in tandem with a *Real-Time Market (RTM)*, both managed by an *Independent System Operator (ISO)*.<sup>1</sup> The primary purpose of the DAM/RTM is to procure sufficient generation to permit the continual balancing of *net load*, i.e., power withdrawal net of *non-dispatchable generation (NDG)*. Below we provide a brief overview of ERCOT DAM/RTM operations.

Market participants in the ERCOT DAM and RTM are represented by *Qualified Scheduling Entities (QSEs)*. Subject to requirements explained in

---

<sup>1</sup>Roughly stated, *independence* means that the ISO is prohibited from having any material or financial stake in market operations that could hinder its ability to carry out its management duties in an impartial manner.

[29, 30], QSEs can submit offers into the DAM/RTM to sell energy and ancillary services as well as bids into the DAM/RTM to buy energy.

The ERCOT DAM is a forward market with a day-ahead planning horizon [29]. During the morning of each day D, the ISO receives bids and offers from participant QSEs. The ISO then conducts a DAM SCUC/SCED<sup>2</sup> optimization, conditional on ISO forecasted NDG, to determine QSE unit commitments, ancillary services, cleared bids, and a generation dispatch schedule for day D+1.

The ERCOT RTM is a balancing mechanism [30]. It consists of multiple sub-markets with shorter look-ahead horizons whose purpose is to reduce discrepancies between DAM generation dispatch schedules and actual real-time net loads.

More precisely, as detailed in [30, sec. 6.3], the ERCOT RTM for an operating hour H on day D+1 runs from the close of the DAM on day D to one hour prior to H, an interval of time called the *Adjustment Period* for H. QSEs submit offers and price-sensitive bids into the ERCOT RTM during this Adjustment Period. At the close of this Adjustment Period the ERCOT ISO conducts an RTM SCED optimization to determine which QSE-submitted offers/bids to clear for H, conditional on ISO-forecasted fixed load, ISO-forecasted NDG, and operating conditions for H.

During the hour between the end of the Adjustment Period and the start of the operating hour H, the ERCOT ISO undertakes various additional preparatory actions in advance of H operations. Finally, during H itself, ERCOT conducts a SCED optimization at least once every 5 minutes to ensure that any changes in forecasts and operating conditions are accounted for in its subsequent dispatch instructions for H.

ERCOT DAM settlements for scheduled generation (MW) are determined by means of *Locational Marginal Prices (LMPs)* (\$/MWh), i.e., the pricing of power in accordance with the location and timing of its injection into, or withdrawal from, a physical grid. LMPs are dual variable solutions for SCED optimizations, given SCUC-optimized unit commitments. The LMP for a grid location b during hour H of day D+1 is the dual variable of the power balance constraint for b during H, calculated at the SCED optimal

---

<sup>2</sup>SCUC is an acronym for *Security-Constrained Unit Commitment*, and SCED is an acronym for *Security-Constrained Economic Dispatch*.



solution point.<sup>3</sup>

Similarly, ERCOT DAM settlements for ancillary services (MW) are determined by means of a *Market Clearing Prices for Capacity (MCPC)* (\$/MW) determined at specific grid locations for specific hours. MCPCs are dual variable solutions for SCED optimizations, conditional on SCUC-optimized unit commitments. The MCPC for a specific type of ancillary service at a grid location  $b$  during hour  $H$  of day  $D+1$  is the dual variable of the requirement constraint for this ancillary service at location  $b$  during hour  $H$ , calculated at the SCED optimal solution point.

The RTM and operating-hour SCED optimizations conducted for a specific operating-hour  $H$  during day  $D+1$  indicate whether any changes are needed in the generation scheduled in the day- $D$  DAM at specific grid locations during hour  $H$ . Any such changes are settled in accordance with time-weighted averages of the LMPs determined in these SCED optimizations for these grid locations.

### 3.2. ERCOT DAM/RTM Supply Offers

ERCOT DAM/RTM supply offers are carefully explained in [29, 30]. Apart from time-scale, the supply offers that QSEs are permitted to submit into the ERCOT RTM are similar in form to the supply offers that QSEs are permitted to submit into the ERCOT DAM. For concreteness, the remainder of this section focuses on ERCOT DAM supply offers.

ERCOT permits QSEs to submit hourly energy supply offers into the ERCOT DAM for all twenty-four hours  $H$  of the following day. For a currently off-line QSE, each such offer typically consists of three parts: a *Startup Offer* (\$/start); a *Minimum-Energy Offer* consisting of a price (\$/MWh) together with a power level (MW) referred to as a *Low Sustained Limit (LSL)*; and a non-decreasing piecewise linear *Energy Offer Curve* in the MW-\$/MWh plane consisting of a finite collection of linearly-connected dispatch points  $dp(H)$  whose power levels commence at LSL.<sup>4</sup>

---

<sup>3</sup>The dual variable for any constraint appearing among the system constraints for a SCED optimization measures the change in the optimized value of the SCED objective function with respect to a change in the constraint constant for this constraint, calculated at an optimal SCED solution point. See [31, 32] for detailed discussions of the mathematics of dual variable determination in U.S. ISO/RTO-managed wholesale power markets.

<sup>4</sup>A QSE can submit an Energy Offer Curve without a Minimum Energy Offer and/or a Startup Offer. However, a QSE cannot submit a Minimum Energy Offer and/or a Startup

QSEs can also submit hourly ancillary service *block offers* into the ERCOT DAM for each hour of the following day. A block offer consists of a single price (\$/MW) and quantity (MW), where the offered quantity can be a fixed MW level or an upper limit (MW) for a range of MW levels.

Suppose an off-line QSE at a grid location  $b$  submits a three-part supply offer into the ERCOT DAM on day  $D$  for hour  $H$  of day  $D+1$ . The Startup Offer permits the QSE to report its start-up cost  $SUC(b,H)$  (\$) for hour  $H$  (if any). The Minimum-Energy Offer permits the QSE to report its minimum-energy cost  $MEC(b,H)$  (\$) for hour  $H$  (if any).<sup>5</sup> The Energy Offer Curve permits the QSE to report, in approximate form, its marginal production cost curve for injected power at grid location  $b$  during hour  $H$ .

Suppose the QSE is scheduled for a particular dispatch point  $dp^*(b,H)$  at grid location  $b$  for hour  $H$  of day  $D+1$  by a SCUC/SCED optimization conducted for the ERCOT DAM on day  $D$ . The day- $D$  DAM settlement received by the QSE for hour  $H$  of day  $D+1$  is then calculated as follows.

First, the QSE is paid the DAM LMP (\$/MWh) determined at grid location  $b$  for hour  $H$  of day  $D+1$  for each MWh of its scheduled energy delivery at  $b$  during hour  $H$  of day  $D+1$ ; let this LMP be denoted by  $LMP(b,H)$ . The resulting energy payment (\$) is the QSE's *Energy Revenue* at bus  $b$  for hour  $H$ , denoted below as  $ER(b,H)$ .<sup>6</sup> For example, suppose the QSE's dispatch set point at bus  $b$  for hour  $H$  is  $dp^*(b,H) = (80\text{MW}, \$40/\text{MWh})$ , and  $LMP(b,H) = \$50/\text{MWh}$ . Then the QSE's scheduled energy delivery at  $b$  for hour  $H$  would be  $80\text{MW} \times 1 \text{ hour}$ , and its energy payment would be  $80\text{MWh} \times \$50/\text{MWh} = \$4,000$ .

Next, the QSE's Energy Offer Curve is used to calculate the QSE's *Average Incremental Energy Cost (AIEC)*, an approximation for the QSE's true production cost for its scheduled energy delivery at its grid location  $b$  during hour  $H$ ; see [29, Sec. 4.6.5] for AIEC calculation details. Let this

---

Offer without also submitting an Energy Offer Curve.

<sup>5</sup> $MEC(H)$  can include the cost of behind-the-meter power generated by the QSE during hour  $H$  to maintain itself in a synchronized state.

<sup>6</sup>Note that  $ER(b,H)$  depends only on the QSE's total scheduled energy delivery at bus  $b$  during hour  $H$ , not on the particular power path used within  $h$  by the QSE to achieve this energy delivery. As emphasized in [27, Module 3, p. 12], the ERCOT DAM does not consider ramp-rates; it is the responsibility of the individual participant QSEs to manage their ramp constraints in order to fulfill their scheduled energy delivery obligations as closely as possible.

approximate production cost be denoted by  $AIEC(b,H)$  (\$). The true total cost (\$) that the QSE would have to incur to fulfill its scheduled energy delivery obligations at grid location  $b$  during hour  $H$  of day  $D+1$  is then approximated as  $TC(b,H) = SUC(b,H) + MEC(b,H) + AIEC(b,H)$ .

Finally, Let  $ASR(b,H)$  (\$) denote the *Ancillary Service Revenue* that is awarded to the QSE for hour  $H$ . If  $TC(b,H) > ER(b,H) + ASR(b,H)$ , the QSE receives a *Make-Whole-Payment* (\$) equal to  $[TC(b,H) - ER(b,H) - ASR(b,H)]$  in addition to  $ER(b,H) + ASR(b,H)$ .<sup>7</sup> Otherwise, the QSE receives  $ER(b,H) + ASR(b,H)$ .

### 3.3. ERCOT DAM/RTM Energy Bids

ERCOT permits QSEs to submit price-responsive energy bids into its DAM. In addition, ERCOT permits QSEs to submit price-responsive energy bids into its RTM if these bids are on behalf of *Load-Serving Entities (LSEs)* representing *Controllable Load Resources (CLRs)*. ERCOT [30] defines a CLR to be a load with installed real-time telemetry that can incrementally increase or decrease its power usage in response to dispatch instructions (“base points”) received from its controlling QSE. Each DAM/RTM price-responsive energy bid consists of a maximum of ten price-quantity pairs with monotonically non-increasing not-to-exceed prices (\$/MWh) and with increasing quantities (MW).

ERCOT also permits QSEs to submit fixed (non-price-responsive) energy bids into its DAM, but not into its RTM. A fixed energy bid submitted into the ERCOT DAM on day  $D$  consists of a 24-hour load profile for day  $D+1$ .

Additional specialized requirements separately imposed on DAM energy bids and RTM energy bids are given in [29, Sec. 4.4.9.6] and [30, Sec. 6.4.3.1], respectively.

## 4. ERCOT Test System: Market Component

### 4.1. Overview

The wholesale power market component for the ERCOT Test System is implemented by means of AMES V5.0 [18, 19]. As depicted in Fig. 1, AMES (*Agent-based Modeling of Electricity Systems*) models core features

---

<sup>7</sup>As detailed in [33], make-whole payments in existing ISO-managed wholesale power markets such as ERCOT can also include side-payments for lost opportunity cost arising from the non-convexity of a generation resource’s true total cost function.

of actual U.S. ISO/RTO-managed wholesale power markets, such as ERCOT. This section provides a summary description of these core market features.

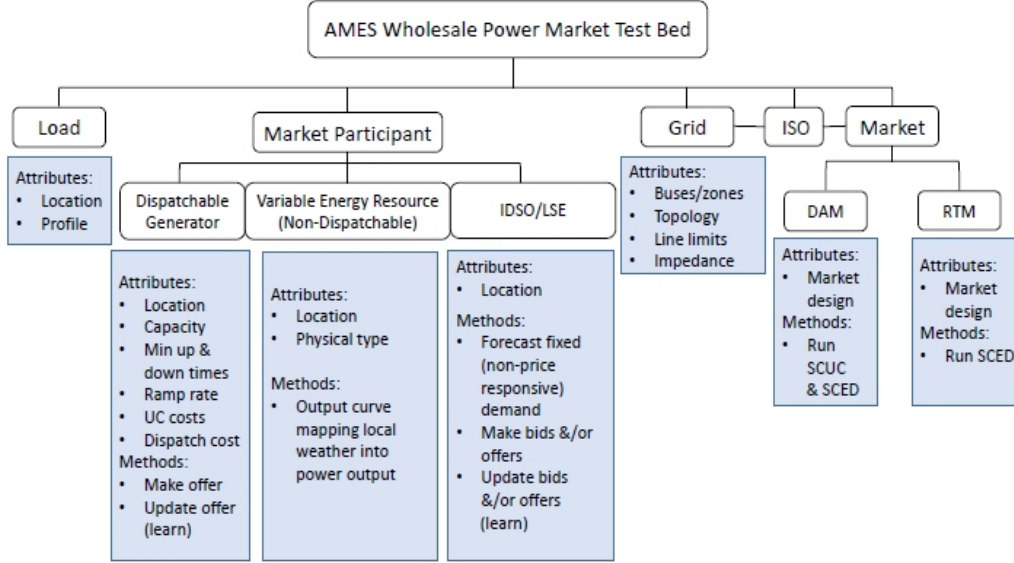


Figure 1: *Partial agent hierarchy for AMES V5.0*

#### 4.2. Core Implemented Market Features

The wholesale power market operates over an AC transmission grid for MaxDay successive days. Each simulated day  $D$  consists of 24 successive hours  $H = 1, 2, \dots, 24$ .

The wholesale power market includes a daily ISO-managed DAM and multiple daily ISO-managed RTMs. Fig. 2 indicates how the ERCOT Test System implements timing for a general market  $M(T)$  corresponding to a future operating period  $T$ , with a look-ahead horizon  $LAH(T)$ . Fig. 3 depicts how the ERCOT Test System implements timing for the DAM. Fig. 4 depicts how the ERCOT Test System implements timing for the RTM; a user can override these default RTM timing settings with user-set values if desired.<sup>8</sup>

<sup>8</sup>As discussed in Section 3, ERCOT in fact conducts an RTM SCED optimization one hour in advance of each operating hour  $H$ . However, ERCOT also conducts additional SCED optimizations at least once every five minutes during  $H$  on the basis of continually updated forecasts for net load and system operating conditions. Users can configure

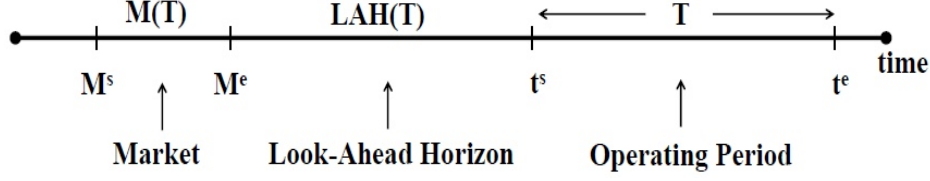


Figure 2: *ERCOT Test System timing configuration for a general market  $M(T)$  whose purpose is to facilitate net load balancing during a future operating period  $T$*

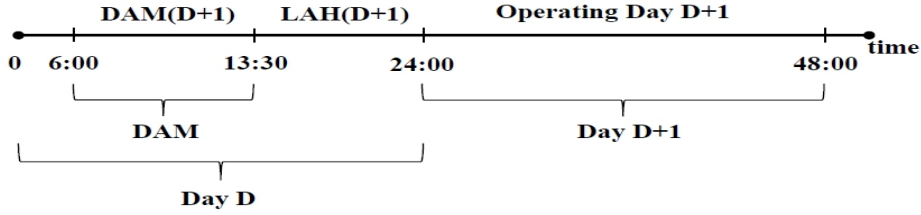


Figure 3: *ERCOT Test System timing configuration for a DAM conducted on day  $D$  to facilitate net load balancing during the following day  $D+1$*

The fiduciary objective of the ISO is to maximize the total net benefit of the market participants, subject to system constraints. The market participants include:<sup>9</sup> (i) a collection of private profit-seeking dispatchable generators; (ii) a collection of private profit-seeking LSEs servicing the power usage needs of retail customers; and (iii) a collection of private profit-seeking non-dispatchable generators (e.g., solar PV and wind farms). *Net benefit* is measured as expressed willingness to pay for resources minus resource procurement costs.

The ISO conducts a daily DAM for next-day operations. The ISO clears each DAM by means of a SCUC/SCED optimization.<sup>10</sup> The inputs for a DAM SCUC/SCED optimization include generator supply offers, LSE price-

---

the ERCOT Test System to implement these more computationally intensive real-time operations if needed for their research purposes.

<sup>9</sup>As discussed in Section 3, ERCOT requires *Qualified Scheduling Entities (QSEs)* to submit bids and offers on behalf of ERCOT market participants. The ERCOT Test System omits this mediation layer since it does not affect market outcomes.

<sup>10</sup>A complete analytical representation for this ISO-managed SCUC/SCED optimization is provided in Tesfatsion and Battula [18].

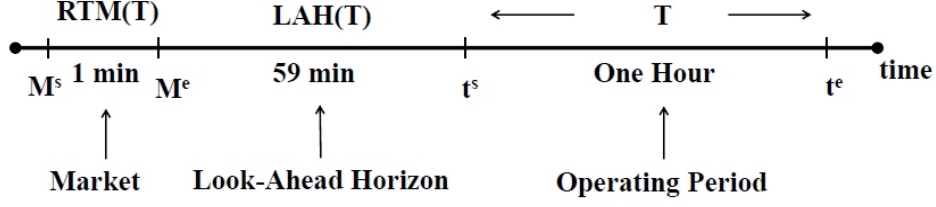


Figure 4: *ERCOT Test System default timing configuration for an RTM whose purpose is to facilitate net load balancing for a near-term operating hour  $T$*

sensitive and/or fixed (non-price-sensitive) demand bids, and ISO NDG forecasts for next-day operations. The system constraints include:

- transmission line power flow limits;
- power balance constraints;
- generator capacity constraints;
- dispatchable generator ramp constraints for start-up, normal, and shut-down operating conditions;
- dispatchable generator min up/down-time constraints;
- dispatchable generator hot-start constraints;
- system-wide reserve requirement constraints;
- zonal reserve requirement constraints.

The outcomes of a DAM SCUC/SCED optimization include generator unit commitments, reserve procurement, a generation dispatch schedule, and cleared LSE price-sensitive demands for next-day operations. LMPs (power balance dual variables) and MCPCs (reserve constraint dual variables) are determined by conducting a secondary SCED optimization, conditional on the optimal unit commitments determined in the original DAM SCUC/SCED optimization.

The ISO also conducts an RTM one hour in advance of each operating hour. The ISO clears each RTM by means of a SCED optimization. The

inputs for an RTM SCED optimization for an operating hour  $H$  include: generator supply offers for  $H$ , LSE price-sensitive demand bids for  $H$ , ISO fixed load forecasts for  $H$ , and ISO NDG forecasts for  $H$ . The system constraints for the RTM SCED optimization are the same as for the DAM SCED optimization. The outcomes of an RTM SCED optimization include reserve procurements, a generation dispatch schedule, cleared LSE price-sensitive demands, LMPs, and MCPCs for the operating hour  $H$ .

The DAM/RTM SCED optimizations have a standard DC Optimal Power Flow (DC-OPF) form [11]. Consequently, they rely on the following three assumptions. First, the resistance for each transmission line is negligible compared to the reactance, hence the resistance for each transmission line can be set to 0. Second, the voltage magnitude at each bus is equal to a common base voltage magnitude. Third, the voltage angle difference  $\Delta\theta(\ell)$  across any line  $\ell$  is sufficiently small that the following approximations can be used:  $\cos(\Delta\theta(\ell)) \approx 1$  in size and  $\sin(\Delta\theta(\ell)) \approx \Delta\theta(\ell)$  in size.

## 5. ERCOT Test System: Grid Component

### 5.1. Overview

The implementation of ERCOT test cases by means of the ERCOT Test System requires the construction of synthetic transmission grids. In this section we present a systematic method for carrying out this grid construction, a variant of the approach developed in [20]–[26]. This method consists of the following six steps:

- (i) Specify the desired number  $NB$  of buses for the grid;
- (ii) Obtain ERCOT generation and load data;
- (iii) Use this ERCOT data to specify  $NN$  initial pure-generation and pure-load nodes, where  $NN \geq NB$ ;<sup>11</sup>
- (iv) Cluster these initial  $NN$  nodes into  $NB$  node clusters, called “buses”, where the nodes comprising each “bus” can be all pure-generation, all pure-load, or mixtures of the two;

---

<sup>11</sup>Section 6.4 concretely demonstrates this initial-node specification.

- (v) Use a Delaunay Triangulation method to construct initial synthetic transmission lines connecting pairs of the  $NB$  buses constructed in step (iv);
- (vi) Prune the resulting grid to achieve greater empirical realism for the particular application at hand, e.g., remove lines that traverse areas outside the energy region of interest.

Section 5.2 explains the bus construction method described in Step (iv), and Section 5.3 explains the line construction method described in Step (v). The full six-step synthetic grid construction method (i)-(vi) is used in Section 6 to construct an illustrative 8-Bus ERCOT test grid.

### 5.2. Synthetic Bus Construction Method

A modified version of the well-known hierarchical clustering algorithm developed by Johnson [34] is used to implement step (iv) in the five-step synthetic grid construction method described in Section 5.1.

For the application at hand, each cluster is assigned the following two properties: a positive weight ( $P$ ) that indicates the total amount (MW) of generation and load associated with this cluster; and geographical (latitude and longitude) location coordinates  $(lt, lg)$ . Suppose two clusters  $c_1$  and  $c_2$  have properties  $(P_1, lt_1, lg_1)$  and  $(P_2, lt_2, lg_2)$ , respectively. If these two clusters are merged to form a new cluster  $c$ , the properties  $(P, lt, lg)$  for  $c$  are calculated as follows:

$$P = P_1 + P_2 \tag{1}$$

$$lt = \frac{(P_1 \cdot lt_1 + P_2 \cdot lt_2)}{(P_1 + P_2)} ; \tag{2}$$

$$lg = \frac{(P_1 \cdot lg_1 + P_2 \cdot lg_2)}{(P_1 + P_2)} . \tag{3}$$

The distance  $D(c, c')$  between any two clusters  $c$  and  $c'$  is then determined as a function of their geographical coordinates. Specifically, if  $(lt, lg)$  and  $(lt', lg')$  are the geographical location coordinates for clusters  $c$  and  $c'$ , respectively, their distance  $D(c, c')$  is measured as

$$r \cdot \sqrt{\left( (lg' - lg) \cos(0.5[lt' - lt]) \right)^2 + (lt' - lt)^2} \tag{4}$$



where  $r = 3,958.8$  miles approximates the radius of the earth.

*Cluster Algorithm Initialization:*

- *Initial Step 1:* Use ERCOT data to construct a set  $\mathbb{N}_g$  of pure-generation nodes  $n_g$ , each consisting only of generation plants. Let  $NN_g$  denote the cardinality of  $\mathbb{N}_g$ .
- *Initial Step 2:* Use ERCOT data to construct a set  $\mathbb{N}_\ell$  of pure-load nodes  $n_\ell$ , each consisting only of load sources. Let  $NN_\ell$  denote the cardinality of  $\mathbb{N}_\ell$ .
- *Initial Step 3:* Calculate the total generation capacity (MW) of each node  $n_g \in \mathbb{N}_g$  to be the generation capacity summed across all of the generation resources included in  $n_g$ .
- *Initial Step 4:* Calculate the total load (MW) of each node  $n_\ell \in \mathbb{N}_\ell$  to be the load summed across all of the load sources included in  $n_\ell$ .
- *Initial Step 5:* Let  $\mathbb{N} = \mathbb{N}_g \cup \mathbb{N}_\ell$  denote the set consisting of all pure-generation and pure-load nodes. Let  $NN = NN_g + NN_\ell$  denote the cardinality of  $\mathbb{N}$ . Assign properties  $(P_n, lt_n, lg_n)$  to each node  $n \in \mathbb{N}$ .
- *Initial Step 5:* Define a *cluster* to be any subset of  $\mathbb{N}$ .
- *Initial Step 6:* Start with  $NN$  clusters in a cluster vector  $CV(NN) = (c_1, c_2, \dots, c_{NN})$ , where each cluster  $c_n$  consists of a single node  $n$  that is either a pure-generation node from  $\mathbb{N}_g$  or a pure-load node from  $\mathbb{N}_\ell$ .

*Cluster Algorithm Reduction Method:*

We next describe the steps taken to reduce an initial cluster vector  $CV(NN)$  with  $NN$  elements to a cluster vector  $CV(NB)$  with  $NB < NN$  elements, where  $NB$  is the desired number of buses for a synthetic grid.

- *Reduction Step 1:* Select a pair of clusters  $c_i$  and  $c_j$  from the current cluster vector that have minimum distance from each other, and combine these two clusters to form a new cluster  $c_{ij}$ .
- *Reduction Step 2:* Assign properties  $(P, lg, lt)$  to the new cluster  $c_{ij}$ .

- *Reduction Step 3:* Calculate the total generation capacity and total load for the new cluster  $c_{ij}$ .
- *Reduction Step 4:* Remove the clusters  $c_i$  and  $c_j$  from the current cluster vector and replace them with  $c_{ij}$  to form an updated cluster vector whose dimension is reduced by one. Update the pairwise distances between the reduced number of clusters in this updated cluster vector.
- *Reduction Step 5:* Repeat reduction steps 1-4 until a cluster vector  $CV(NB)$  with the required dimension  $NB$  has been formed.
- *Reduction Step 6:* By construction, each of the  $NB$  elements in the final cluster vector  $CV(NB)$  is a cluster of elements from the initial cluster vector  $CV(NN)$ . Each of these  $NB$  elements constitutes a distinct “bus” for the  $NB$ -bus transmission grid.

Reduction Steps 1-6 do not impose any constraints on the *types* of nodes (pure-generation or pure-load) that are included in the clusters selected for combination in Reduction Step 1. Thus, each of the  $NB$  clusters appearing as an element of the final cluster vector  $CV(NB)$  can consist entirely of pure-generation nodes from  $\mathbb{N}_g$ , entirely of pure-load nodes from  $\mathbb{N}_\ell$ , or mixtures of nodes from both  $\mathbb{N}_g$  and  $\mathbb{N}_\ell$ .

### 5.3. Synthetic Line Construction Method

Given a finite set of  $NB$  buses, these buses can be connected by transmission lines in  $NB \cdot [NB - 1]$  different ways. However, not all of the resulting grids have realistic topologies.

As shown in Birchfield et al. [22, 23], a “Delaunay Triangulation” method applied to a finite set of  $NB$  buses spatially located in a plane results in a grid whose connection topology captures several important properties of real-world grids. The method thus provides an excellent starting place for the construction of synthetic grids.

As detailed in [35, Ch. 6], a *triangulation*  $T(\mathbb{S})$  of a point set  $\mathbb{S}$  consisting of finitely many points in the  $R^2$  plane is a collection of triangles (described by edges and vertices) such that: (i) the union of these triangles forms the *convex hull* of  $\mathbb{S}$ , i.e., the smallest convex set that contains  $\mathbb{S}$ ; (ii) the point set  $\mathbb{S}$  equals the union of the vertices of these triangles; and (iii) the intersection

of any two of these triangles is either a common vertex, a common edge, or an empty set.

A *circumcircle* of a triangle in the  $R^2$  plane is a circle in the  $R^2$  plane whose circumference passes through all three vertices of this triangle.<sup>12</sup> Finally, a triangulation  $T(\mathbb{S})$  of a point set  $\mathbb{S}$  consisting of finitely many points in the  $R^2$  plane is said to be a *Delaunay Triangulation* of  $\mathbb{S}$ , denoted by  $DT(\mathbb{S})$ , if no point in  $\mathbb{S}$  lies strictly within the circumcircle of any triangle in  $T(\mathbb{S})$ ; see Fig. 5. As established in [35, Secs. 6.2-6.4], a finite point set  $\mathbb{S}$  in the  $R^2$  plane whose points do not all lie on a common line has at least one Delaunay Triangulation.

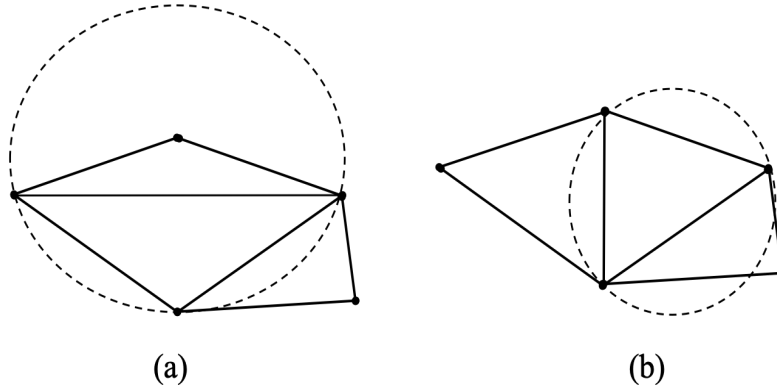


Figure 5: (a) The depicted grid is not a Delaunay Triangulation of the five indicated buses because at least one triangle's circumcircle includes a bus within its interior. (b) The depicted grid is a Delaunay Triangulation of the five buses in (a) because there does not exist any triangle with a circumcircle that contains a bus within its interior. Adapted from [22, Fig. 5].

Birchfield et al. [22] report that the number  $m$  of transmission lines found in North American interconnected transmission grids approximately satisfies  $m = 1.22NB$ , where  $NB$  is the number of grid buses. On the other hand,

<sup>12</sup>Every triangle in the  $R^2$  plane that encloses a positive area has a unique circumcircle. The geometric proof of this claim proceeds by establishing that each such triangle has a unique *circumcenter*  $p$ , i.e., a unique point in the  $R^2$  plane where the perpendicular bisectors of its sides intersect. By construction,  $p$  is at an equal distance  $r$  from each of the triangle's three vertices. The circle with center point  $p$  and radius  $r$  constitutes the unique circumcircle for the triangle.

the number of lines produced by a Delaunay Triangulation applied to a finite point set  $\mathbb{B}$  consisting of  $NB$  synthetic buses in the  $R^2$  plane is  $NL(\mathbb{B}) = 3NB - k - 3$ , where  $k$  denotes the number of points from  $\mathbb{B}$  that lie on the outer edges of the convex hull of  $\mathbb{B}$ ; see [35, Lemma 6.4]. Birchfield et al. [22] reason that  $NL(\mathbb{B})$  is relatively close to  $1.22NB$ , given that the total number of possible lines connecting the  $NB$  buses is  $NB \cdot [NB-1]$ .

Many suggestions for improving the realism of the synthetic grids resulting from application of the Delaunay Triangulation method to a finite bus set are discussed in Birchfield et al. [23, 24]. For example, the authors note that the incorporation of a DC power flow analysis within the procedure for generating the synthetic grid lines can increase the chances that the resulting synthetic grid will have convergent AC power flow solutions [23]. Moreover, further realism of the resulting synthetic grid can be obtained by incorporating additional features such as phase-shifting transformers, multiple areas with different nominal voltage levels, and multiple reactive power devices remotely regulating a single bus voltage [24].

## 6. An Illustrative 8-Bus ERCOT Test Grid

### 6.1. Overview

This section describes the construction of a synthetic 8-bus ERCOT test grid that can be used for DC optimal power flow and DC power flow analyses for which voltage problems are not an issue. The resulting grid, referred to as the *8-Bus ERCOT DC Test Grid*, is suitable for exploratory studies of transactive market mechanisms.

The section first describes the generation, weather zone, and population data used to construct the 8-Bus ERCOT DC Test Grid. It then describes the synthetic construction of buses and transmission lines for this grid.

### 6.2. ERCOT Generation Data

The ERCOT generator data used to construct the 8-Bus ERCOT DC Test Grid were obtained from the U.S. Energy Information Administration (EIA) [36]. The vast data in these files were searched to obtain pertinent information about generation resources located within the ERCOT region of Texas. To help ensure the completeness of this generation data, we focused on data for 2016.

Below we provide a brief summary of the ERCOT generation data we obtained for 2016:

- The state of Texas had 1040 generators in operation, 834 of which were located in the ERCOT energy region.
- For each ERCOT generator we obtained its designated location (latitude and longitude), nameplate capacity, and fuel type.
- The capacity proportions of the 834 ERCOT generators, by fuel type,<sup>13</sup> are reported in Fig. 6.
- Major fuel-type generation (natural gas 58%, conventional steam coal 20%, onshore wind 15%, nuclear 5%, solar photovoltaic 1%) constituted approximately 99% of total 2016 ERCOT generation capacity.

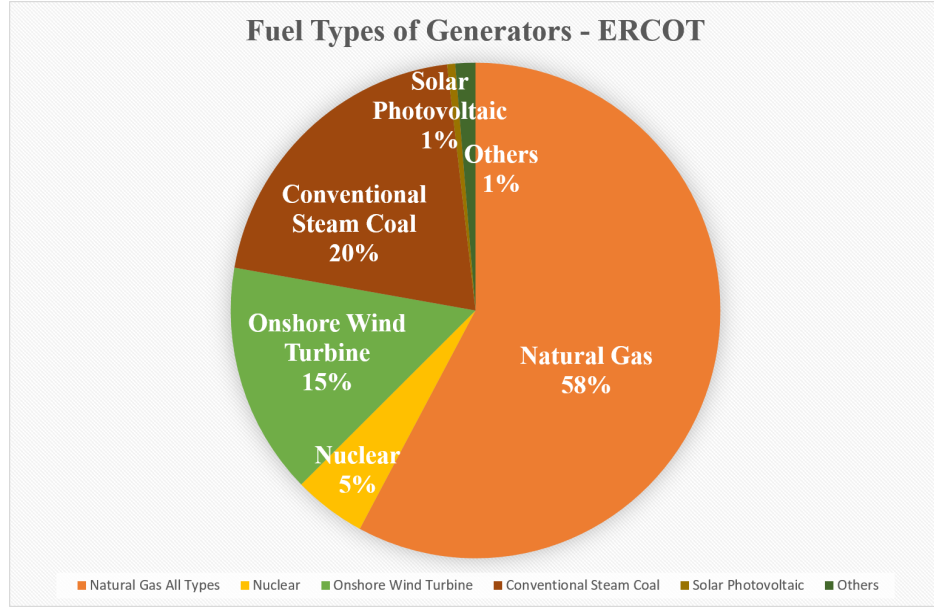


Figure 6: *ERCOT 2016 generation capacity proportions by major fuel types*

Only major fuel-type generation is taken into consideration in the formation of the 8-Bus ERCOT DC Test Grid.

<sup>13</sup>The capacity proportions for major fuel-type generators are reported separately. The aggregated capacity proportion for all non-major fuel-type generators is reported under the ‘Others’ category. These non-major fuel types include conventional hydroelectric, batteries, wood, wood waste biomass, other waste biomass, petroleum liquids, petroleum coke, landfill gas, and other gas types.

### 6.3. ERCOT Weather Zone and Population Data

As depicted in Fig. 7, ERCOT has eight weather zones [37]. Each weather zone represents a geographic region with similar climate characteristics. Table 2 reports the average hourly per-capita power consumption level we assigned to each of these eight weather zones for 2016, using values adapted from [23, Table IV]. Finally, 2016 population data for ERCOT by zip code were obtained from U.S. Census data [38].



Figure 7: *ERCOT weather zones. Public source: ERCOT.com*

### 6.4. Bus Construction for the 8-Bus ERCOT DC Test Grid

The method presented in Section 5.2 for synthetic bus construction requires an initial determination of pure generation nodes and pure load nodes. These nodes were determined as follows for the 8-Bus ERCOT DC Test Grid.

Each pure generation node was formed using geographical location coordinates and generation capacity information for major-fuel-type generators in operation in ERCOT during 2016; see Section 6.2. For this purpose, NDG was treated the same as dispatchable generation. For each ERCOT zip code, a pure load node was formed using the geographical location coordinates and population information for this zip code. The load for this pure-load node

Table 2: 2016 average hourly per-capita power consumption levels assigned to the eight ERCOT weather zones

Weather Zone	Per-capita consumption (kW)
Coast	2.362
East	1.563
Far West	1.854
North Central	2.438
North	1.859
South Central	2.045
Southern	1.843
West	2.368

was set equal to the product of the population reported for the zip code and the average hourly per-capita power consumption level assigned in Table 2 to the weather zone that includes this zip code. Figure 8 depicts the resulting collection of pure generator nodes and pure load nodes. In this figure the red circles represent pure load nodes and the circles with other colors represent pure generator nodes differentiated by fuel type.<sup>14</sup>

The clustering algorithm presented in Section 5.2 was then used to cluster these initial nodes into  $NB=8$  node clusters (“buses”) for the 8-Bus ERCOT DC Test Grid. As will be seen in Section 6.5, each of the resulting eight buses has a mixture of generation and load.

#### 6.5. Line Construction for the 8-Bus ERCOT DC Test Grid

Following the construction of the eight buses for the 8-Bus ERCOT DC Test Grid, the Delaunay Triangulation method described in Section 5.3 was applied to build the line topology. Given the relatively small size of this synthetic grid, no additional DC power flow analysis was performed to further reduce the number of transmission lines. However, three lines along the

---

<sup>14</sup>The specific colors used in Fig. 8 for major generator fuel types are as follows: coal-brown; wind-ink blue; nuclear-dark green; solar PV-blue; and natural gas fired combustion turbine-yellow/orange.

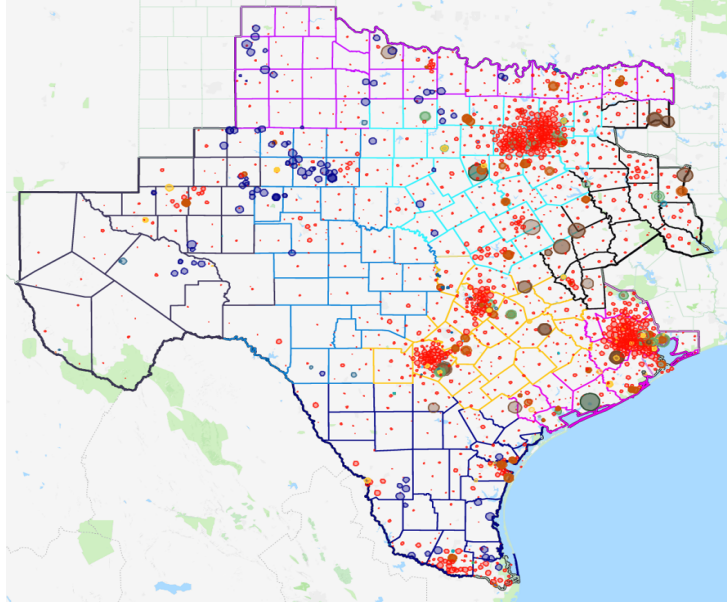


Figure 8: *Pure load nodes (red) and pure generation nodes (colored by fuel type) used to initialize bus construction for the 8-Bus ERCOT DC Test Grid*

southern and western borders were trimmed for greater realism.<sup>15</sup>

Fig. 9 displays the resulting 8-Bus ERCOT DC Test Grid in schematic form. Fig. 10 displays this grid as an overlay of the ERCOT energy region. Table 3 gives the transmission line parameter settings for the 8-Bus ERCOT DC Test Grid, including the *number of parallel lines (NPL)* connecting each pair of buses. All lines are assumed to be 345 kV lines. Each line has a 1084 MVA transmission capacity with a line impedance per mile equal to 0.584 ohms. Parallel lines are used to model higher transmission capacities between bus pairs. For each pair of buses, the indicated line capacity (linCap) and reactance ( $X$ ) are for *each* parallel line between these two buses. Note, also, that the reactance for each parallel line incorporates the length of this line; that is, this reactance is *not* per mile.

---

<sup>15</sup>Specifically, the three removed lines were edges connecting bus 8 to bus 6, bus 8 to bus 7, and bus 8 to bus 3.



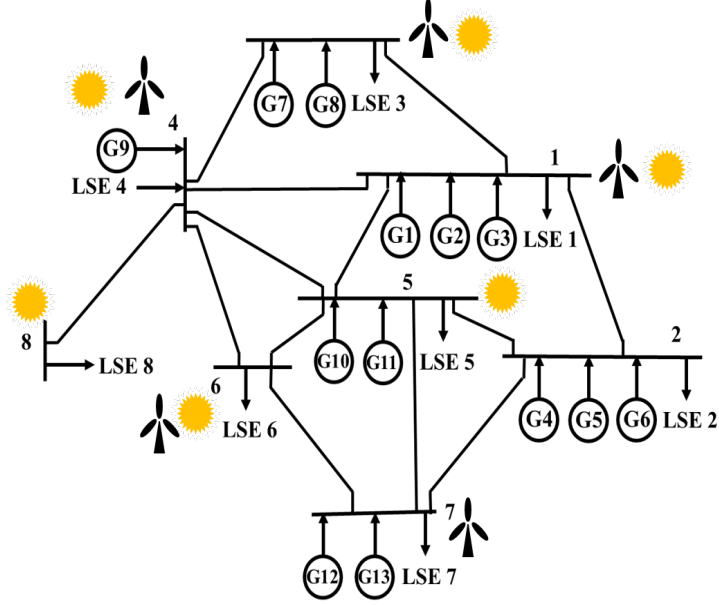


Figure 9: 8-Bus ERCOT DC Test Grid: Schematic rendering that depicts the grid locations of thermal generators ( $G$ ), wind farms (turbines), solar photovoltaic resources (sunbursts), and load-serving entities ( $LSE$ ).

## 7. Application: An 8-Bus ERCOT Test Case

### 7.1. Overview

This section describes an illustrative 8-bus ERCOT test case<sup>16</sup> implemented by means of the ERCOT Test System developed in Sections 4 and 5. Test case outcomes are reported in the following Section 8.

The test case simulates ERCOT's DAM and RTM operating in tandem over an 8-bus transmission grid during successive days. The timing for these DAM and RTM operations is as depicted in Figs. 3-4.

More precisely, a DAM SCUC/SCED optimization is conducted daily for five successive test-case days labeled D0 through D4. The DAM optimization held on each test-case day  $D$  is conditional on dispatchable generator supply offers, LSE fixed demand bids,<sup>17</sup> and ISO forecasted NDG for test-case day

<sup>16</sup>Summary listings of the inputs for this 8-bus test case are provided in Appendix D.

<sup>17</sup>As in the actual ERCOT DAM, the ERCOT Test System implemented by AMES V5.0 permits LSEs to submit price-responsive demand bids into the DAM as well as fixed

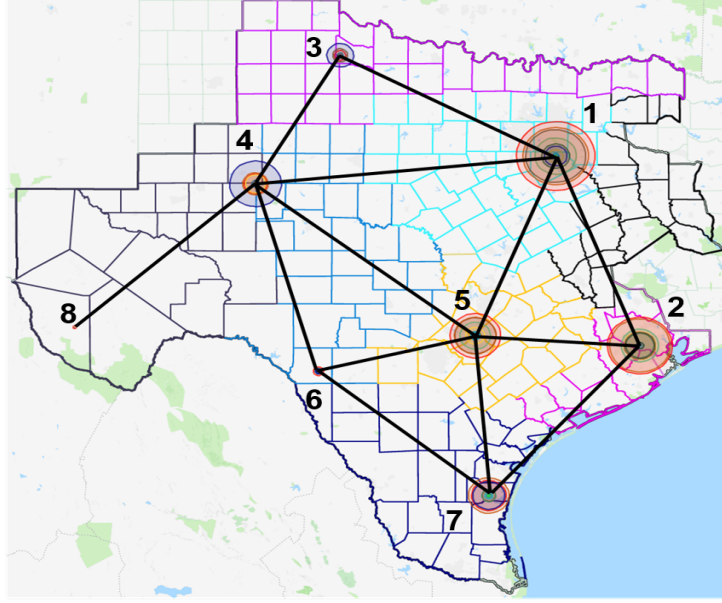


Figure 10: *8-Bus ERCOT DC Test Grid superimposed on the ERCOT region*

D+1. The outcomes of this DAM optimization include bus-distributed DAM LMPs and a bus-distributed generation dispatch schedule for all 24-hours of test-case day D+1.

The RTM is an imbalance mechanism that depends on previous-day DAM outcomes. An RTM SCED optimization is conducted one hour in advance of each operating hour H for test-case days D1 through D5. This RTM optimization is conditional on dispatchable generator supply offers, ISO forecasted load,<sup>18</sup> and ISO forecasted NDG for hour H. The outcomes of this RTM optimization include bus-distributed RTM LMPs and a bus-distributed generation dispatch schedule for hour H. For simplicity, the ISO's forecasted load and forecasted NDG for hour H are assumed to be realized, implying

---

demand bids. However, the 8-Bus ERCOT DC Test Case assumes all DAM LSE demand bids take a fixed form.

<sup>18</sup>As in the actual ERCOT RTM, the ERCOT Test System implemented by AMES V5.0 permits LSEs to submit price-responsive demand bids into the RTM on behalf of customers with dispatchable price-sensitive power demands; LSE fixed demand bids are not permitted. However, the 8-Bus ERCOT DC Test Case assumes that LSEs do not participate at all in the RTM.

Table 3: Transmission line settings for the 8-Bus ERCOT DC Test Grid.

Line		lineCap (MVA)	$X$ (ohms)	Length (Miles)	NPL
From	To				
1	2	1084	122.3124	209.4390	2
1	3	1084	125.6020	215.0720	3
1	4	1084	156.4805	267.9461	2
1	5	1084	116.1924	198.9595	2
2	5	1084	87.7518	150.2599	6
2	7	1084	123.4350	211.3613	2
3	4	1084	87.2334	149.3723	2
4	5	1084	147.8132	253.1047	6
4	6	1084	118.7483	203.3361	2
4	8	1084	126.8891	217.2758	2
5	6	1084	84.1587	144.1073	2
5	7	1084	98.6619	168.9416	2
6	7	1084	118.0990	202.2244	2

that the RTM generation dispatch schedule for hour  $H$  is also realized.

The 8-Bus ERCOT DC Test Grid constructed in Section 6 is used for the transmission grid; hence, the test case is hereafter referred to as the *8-Bus ERCOT DC Test Case*. As seen in Section 6, the construction of the 8-Bus ERCOT DC Test Grid relies on ERCOT generator fuel-type data, ERCOT load data, and settings for line capacities, line lengths, and line reactances. For simplicity, the test case configures this grid into a single reserve zone consisting of the set of all buses. The down/up reserve requirements for this single system-wide reserve zone are commonly set at 10% for the DAM and 1% for the RTM.

The next three subsections explain the following additional inputs for the 8-Bus ERCOT DC Test Case:

- Dispatchable generator attributes
- Non-dispatchable generation: Data Input
- DAM LSE bids and RTM ISO load forecasts: Data Input

The final subsection provides software implementation details.

## 7.2. Dispatchable Generator Attributes

As depicted in Fig. 9, the 8-Bus ERCOT DC Test Case has thirteen dispatchable generators  $\{G1, \dots, G13\}$  distributed across the eight buses of the transmission grid. Each generator  $g$  is distinguished by its fuel type, capacity, no-load cost, and variable cost attributes. The specific settings for these attributes, reported below, are adapted from the settings derived in [17] for an 8-bus test system using ISO New England generator data [39] differentiated by fuel type.

The production cost function (\$/hour) for each of the thirteen dispatchable generators  $g$  is a convex non-decreasing function of  $g$ 's power level  $p$  taking the following quadratic form:

$$C_g(p) = a_g + b_g p + c_g p^2, \quad (5)$$

where  $a_g$ ,  $b_g$ , and  $c_g$  are non-negative coefficients. For simplicity, the range of feasible power levels for each  $g$  is assumed to take the form  $[0, P_g^{\max}]$ .<sup>19</sup> The test-case settings for dispatchable generator bus locations, fuel types, no-load costs  $a_g$ , variable cost coefficients  $\{b_g, c_g\}$ , and maximum power capacities  $P_g^{\max}$  are given in Table 4.

If  $P_g^{\max}$  exceeds 1000MW for some dispatchable generator  $g$ , this generator is implemented as a collection of generation units. Each of these generation units has a minimum feasible power level of 0. Also, each of these generation units has a maximum feasible power level equal to 1000MW, apart from a residual unit whose maximum feasible power level is less than or equal to 1000MW. The sum of the maximum feasible power levels across all generation units associated with  $g$  is equal to  $P_g^{\max}$ . Finally, the cost function for each generation unit associated with  $g$  takes the quadratic form (5), defined over the generation unit's specific feasible power range.

One test-case feature seen in Table 4 that will be of special interest for later reported test-case outcomes is that two of the gas-fired dispatchable generators, G7 and G9, are configured to be *peaker generators*. Specifically, G7 and G9 are fast-start generators with zero no-load cost ( $a=0$ ) and with relatively high marginal costs as indicated by the relatively high settings for their variable-cost coefficients  $b$  and  $c$ .

---

<sup>19</sup>In reality, nuclear units and some coal units have lower power limits  $P^{\min} > 0$ .

Table 4: Dispatchable generator attributes (by fuel type) for the 8-Bus ERCOT DC Test Case

Name	Bus	Fuel Type	$a$	$b$	$c$	$P^{\max}$
G1	1	Natural Gas	2230	35.00	0.00300	19,978.8
G2	1	Coal	2128	19.00	0.00090	11,664.8
G3	1	Nuclear	1250	8.00	0.00019	2,430.0
G4	2	Natural Gas	2230	56.50	0.00750	20,761.7
G5	2	Coal	2128	19.00	0.00090	3,190.3
G6	2	Nuclear	1250	8.00	0.00019	2,708.6
G7	3	Natural Gas	0	57.03	0.00800	80.0
G8	3	Coal	2128	19.00	0.00090	720.0
G9	4	Natural Gas	0	57.03	0.00800	3,438.2
G10	5	Natural Gas	2230	45.00	0.00600	10,589.7
G11	5	Coal	2128	19.00	0.00090	5,728.1
G12	7	Natural Gas	2230	50.00	0.00700	7,385.0
G13	7	Coal	2128	19.00	0.00090	622.4

### 7.3. Non-Dispatchable Generation: Data Input

As depicted in Fig. 9, the 8-Bus ERCOT DC Test Case has NDG (solar PV and wind) distributed across the eight buses of the transmission grid. This test-case NDG has zero marginal cost; and it is represented as negative fixed load in all DAM/RTM SCUC/SCED optimizations.

Table 5 provides installed capacities for this test-case NDG by bus location. These capacities are an outcome of the bus construction method used in Section 6 to construct the 8-Bus ERCOT DC Test Grid. In particular, as explained in Section 6.4, the initial generation nodes used in this bus construction were determined on the basis of 2016 ERCOT generation data available at [36] for NDG as well as for dispatchable generation.

The method used to construct ISO NDG forecasts and NDG realizations for test-case days D1 through D5 on the basis of actual ERCOT data will next be explained. In this explanation, a forecast  $F$  for a test-case day  $D+1$  will be called a *day-ahead forecast* if  $F$  was determined on the previous test-case day  $D$  for use in day- $D$  DAM operations.

Table 5: NDG installed capacities (MW) by bus location for the 8-Bus ERCOT DC Test Case

Bus	Solar	Wind	Bus	Solar	Wind
1	7.0	1,674.8	5	127.5	0.0
2	0.0	0.0	6	139.6	99.8
3	100.0	2,442.2	7	0.0	3,562.2
4	190.2	8,730.3	8	10.0	0.0

Hourly averaged 2019 ERCOT data available at [40] for both day-ahead forecasted NDG and realized NDG were used in scaled bus-distributed form to model ISO NDG day-ahead forecasts and NDG realizations for test-case days D1-D5. Scaling was used in order to reduce these 2019 data to empirically reasonable 2016 magnitudes.

The method used to construct these scaled NDG forecasts and realizations is more carefully explained below:

- Historical ERCOT data for system-wide solar PV and wind profiles in both day-ahead forecasted and realized forms were obtained at [40] for five successive days (07/23/2019 to 07/27/2019) in ‘.xlsx’ format.
- The ratio of installed ERCOT solar PV capacity in 2016 to installed ERCOT solar PV capacity in 2019 is 0.3, and the ratio of installed ERCOT wind capacity in 2016 to installed ERCOT wind capacity in 2019 is 0.7. Thus, the 2019 ERCOT system-wide solar PV and wind profiles were multiplied by 0.3 and 0.7, respectively, in order to obtain scaled ERCOT system-wide NDG load profiles in day-ahead forecasted and realized forms for 2016.
- The scaled ERCOT system-wide *day-ahead forecasted* NDG profiles were used in the test case in bus-distributed form to represent ISO NDG day-ahead forecasts for test-case days D1 through D5.
- The scaled ERCOT system-wide *realized* NDG profiles were used in the test case in bus-distributed form to represent both RTM ISO NDG forecasts and realized NDG outcomes for test-case days D1 through D5. Thus, RTM ISO NDG forecasts are assumed to be accurate.

- The scaled ERCOT system-wide profiles for both day-ahead forecasted NDG and realized NDG were distributed across the eight buses (node clusters) of the test-case grid in proportion to the actual 2016 installed ERCOT solar PV and wind capacity at each bus (node cluster).
- Specifically, the NDG at each bus  $b$  for each test-case hour  $H$ , in both day-ahead forecasted and realized forms, was calculated as follows:

$$[\text{ERCOT NDG for } h] * \frac{[\text{ERCOT NDG capacity at } b]}{[\text{Total ERCOT NDG capacity}]}$$

#### 7.4. DAM LSE Bids and RTM ISO Load Forecasts: Data Input

As depicted in Fig. 9, an LSE is located at each bus of the test-case grid. This LSE manages power usage (withdrawals) at this bus by a collection of retail customers. Each LSE submits into the DAM a fixed demand bid consisting of a 24-hour load profile that represents its forecast for the next-day power usage of its retail customers. However, LSEs do not participate in the RTM; ISO load forecasts take the place of LSE fixed demand bids in the RTM.

Historical ERCOT data for day-ahead load forecasts and load realizations are available at [41]. These data are used in scaled bus-distributed form to model DAM LSE fixed demand bids, RTM ISO load forecasts, and realized load outcomes for test-case days D1 through D5.

More precisely, the method used for these test-case load constructions is as follows. This method is similar to the test-case NDG construction method described in Section 7.3.

- Historical ERCOT data for system-wide load profiles in both day-ahead forecasted and realized forms were obtained at [41] for five successive days (07/23/2019 to 07/27/2019) in ‘.xlsx’ format.
- The ratio of ERCOT average hourly realized load in 2016 to ERCOT average hourly realized load in 2019 is 0.98. Thus, the 2019 ERCOT system-wide load profiles were multiplied by 0.98 to obtain scaled ERCOT system-wide load profiles in day-ahead forecasted and realized forms for 2016.
- The scaled ERCOT system-wide *day-ahead forecasted* load profiles were used in the test case in bus-distributed form to represent LSE day-ahead load forecasts (fixed demand bids) for test-case days D1 through D5.

- The scaled ERCOT system-wide *realized* load profiles were used in the test case in bus-distributed form to represent both RTM ISO load forecasts and realized load outcomes for test-case days D1 through D5. Thus, RTM ISO load forecasts are assumed to be accurate.
- The scaled ERCOT system-wide profiles for both day-ahead forecasted load and realized load were distributed across the eight buses (node clusters) of the test-case grid in proportion to the actual amount of ERCOT load at each bus (node cluster) in 2016.
- Specifically, the load at each bus  $b$  for each test-case hour  $H$ , in both day-ahead forecasted and realized forms, was calculated as follows:

$$[\text{ERCOT load for } h] * \frac{[\text{ERCOT load at } b]}{[\text{Total ERCOT load}]}$$

#### 7.5. Software Implementation

Simulations were carried out by running AMES V5.0 on a machine having 3.5 GHz 4-Core Intel Xeon CPU E3-1240 v5 processor, operating system Windows 10 Enterprise, and 16 GB of RAM. AMES V5.0 uses 64-bit versions of Java (v1.8.0\_161), Python (v3.6.3) and Pyomo (v5.5.0). Pyomo 5.5.0 is used to formulate and solve the DAM SCUC/SCED and RTM SCED market operations. IBM ILOG CPLEX Interactive Optimizer 12.7.1.0 is employed as the *Mixed Integer Linear Programming (MILP)* solver.

### 8. 8-Bus ERCOT DC Test Case Outcomes

This section reports DAM/RTM LMP and scheduled dispatch outcomes for the 8-Bus ERCOT DC Test Case determined for five successive test-case days D1 through D5.<sup>20</sup>

Recall from Sections 7.3 and 7.4 that net load for the test case is implemented as load minus NDG using actual ERCOT load and NDG data in day-ahead forecasted and realized forms. Fig. 11 depicts the day-ahead

---

<sup>20</sup>Recall from Section 7 that the test case is initialized by a test-case day D0 during which only the DAM is conducted, conditional on LSE fixed demand bids (day-ahead load forecasts) and ISO day-ahead NDG forecasts for test-case day D1. The numerical LMP solution values obtained for test-case day D1 in this initial DAM on test-case day D0 are reported in Table 14 in Appendix D.



forecasted net load for test-case days D1-D5, and Fig. 12 depicts the realized net load for test-case days D1-D5.

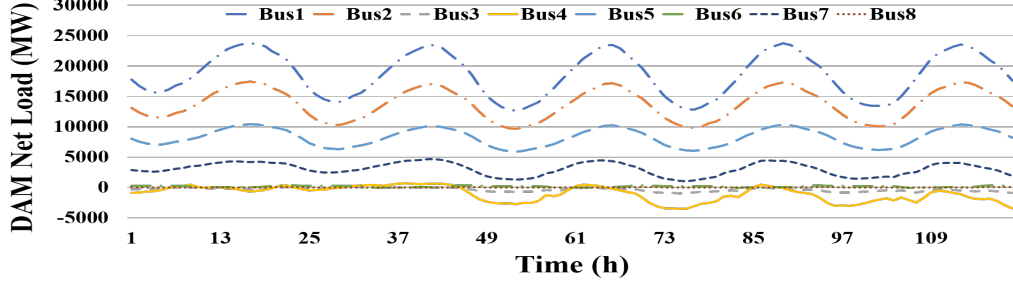


Figure 11: *Day-ahead forecasted hourly net load for test-case days D1-D5*

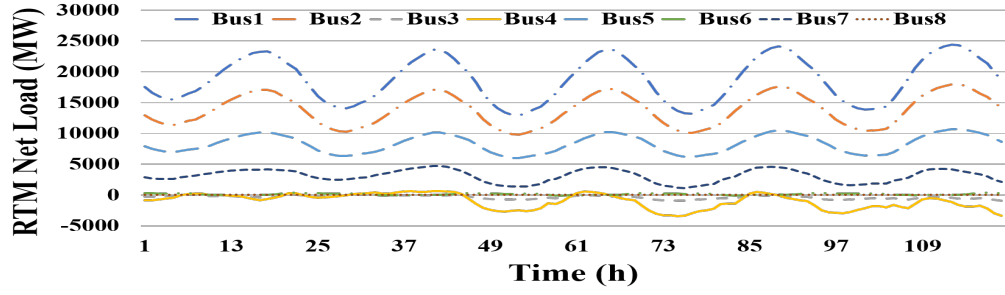
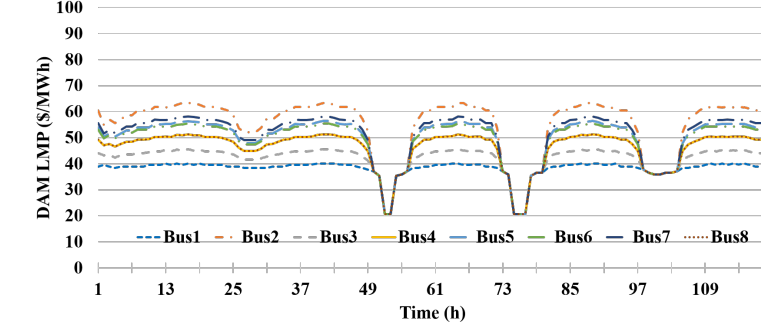


Figure 12: *Realized hourly net load for test-case days D1-D5*

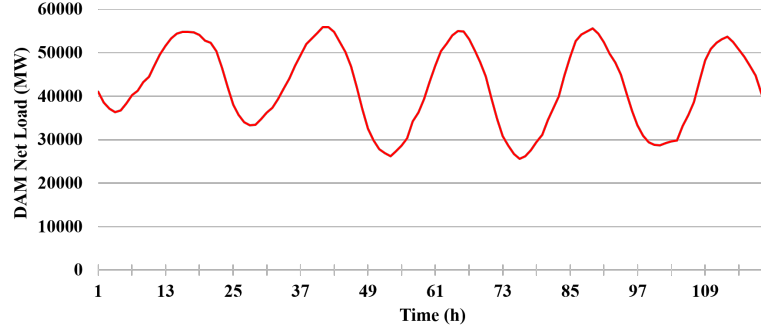
The general pattern displayed by the day-ahead forecasted and realized net load profiles in Figs. 11-12 is similar. Each has an afternoon peak. The maximum deviation between day-ahead forecasted and realized net load is approximately 7%, lower than the 10% down/up reserve requirements assumed for the test-case DAM.

The negative net load (load minus NDG) observed at buses 3 and 4 during some hours arises because wind generation exceeds load. Bus 4 has the highest installed wind capacity (8730.3 MW) across all eight buses, followed by bus 7 (3562.2 MW) and bus 3 (2242.2 MW). Demand at bus 4 is less than wind power during certain hours, resulting in negative net load. Bus 7 has significantly more load than bus 3, resulting in positive net load at bus 7 for all hours and negative net load at bus 3 during some hours.

Fig. 13 depicts the correlation between DAM LMPs and day-ahead forecasted system-wide net load for test-case days D1-D5. The peaks and troughs



(a) *DAM LMPs*



(b) *Day-ahead forecasted system-wide net load*

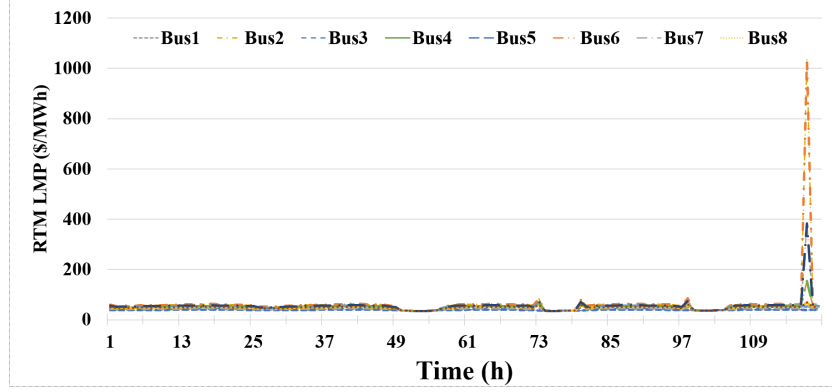
Figure 13: *Correlation between DAM LMPs and day-ahead forecasted system-wide net load for test-case days D1-D5*

in the DAM LMPs are strongly positively correlated with the peaks and troughs in forecasted net load. Note, also, the relatively sharp dips in DAM LMPs during hours 52-53 and 75-77; these dips occur due to relatively sudden increases in forecasted NDG, which has zero marginal cost.

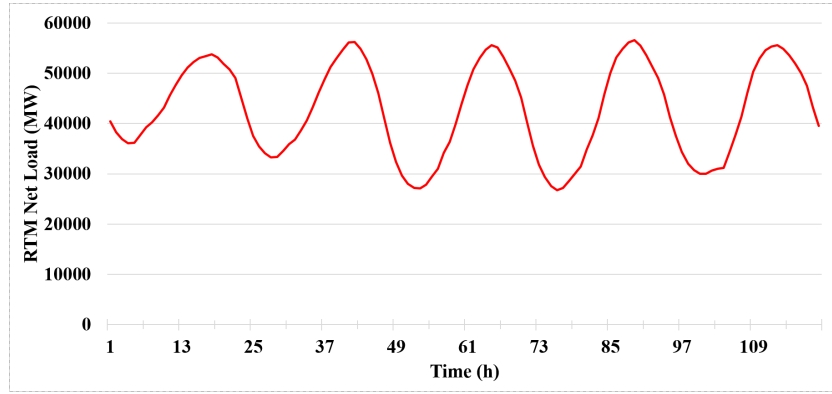
The separation in LMPs across the buses seen in Fig. 13 is due to transmission line congestion. The additional availability of NDG during hours 52-53 and 75-77 results in reduced or eliminated transmission line congestion, hence reduced or eliminated LMP separation across the buses.

Fig. 14 depicts the correlation between RTM LMPs and realized system-wide net load for test-case days D1-D5. Note the very high spike in the RTM LMP that occurs at bus 2 during hour 118, i.e., during the 22nd hour of the final test-case day D5. The explanation for this spike is as follows.

Bus 2 has three dispatchable generators: namely, G4, G5, and G6. In the



(a) *RTM LMPs*



(b) *Realized system-wide net load*

Figure 14: *Correlation between RTM LMPs and realized system-wide net load for test-case days D1-D5*

DAM, G5 and G6 are committed for hour 118; and they are scheduled to generate at their maximum power capacities during hour 118. In contrast, generator G4 does not appear to be needed to ensure the efficient balancing of DAM-forecasted net load during hour 118. Consequently, G4 is not committed in the DAM for hour 118; hence, G4 is not available for dispatch in the RTM for hour 118.

In the RTM, G5 and G6 are again scheduled to generate at their maximum power capacities during hour 118. Thus, these two dispatchable generators are *not marginal* for hour 118; that is, they are *not* able to produce additional generation to balance an incremental increase in fixed load. The RTM LMP at bus 2 for hour 118 is therefore set by marginal generators at other buses,

not by G5 and G6. Moreover, in the RTM solution the lines connecting buses 1 and 2 and buses 2 and 5 are congested during hour 118. These RTM operating conditions require the ISO to resort to out-of-merit order dispatch in order to balance forecasted load at bus 2 during hour 118. The result is a high RTM LMP at bus 2 during hour 118.

The situation is similar for hour 117 with one major exception: namely, G4 is committed in the DAM for hour 117, and is marginal at bus 2 during hour 117 in the RTM. Consequently, the RTM LMP at bus 2 during hour 117 is set by the marginal cost of G4; there is no price spike.

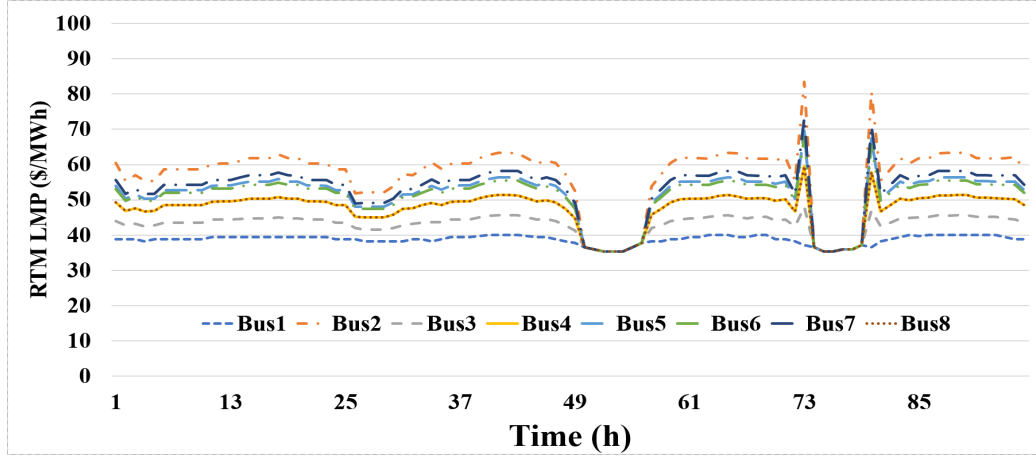
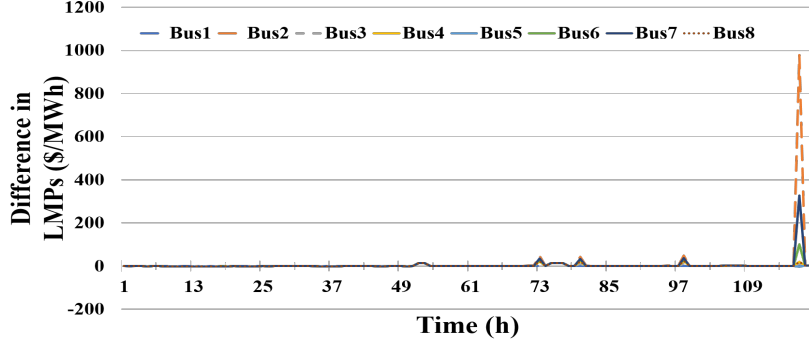


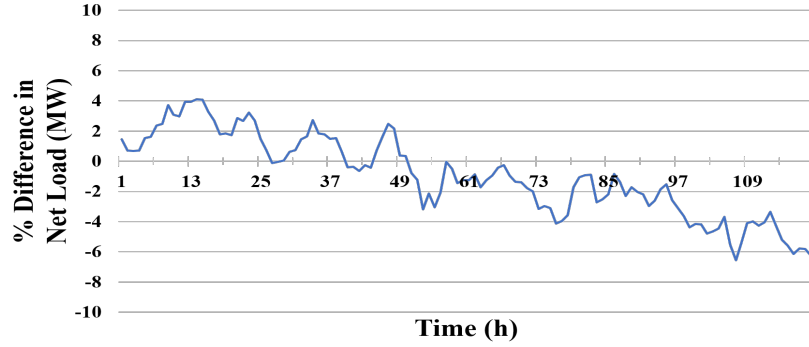
Figure 15: *RTM LMPs for test-case days D1-D4*

The appearance of the dramatic RTM LMP spike during the final test-case day D5, observed in Fig. 14a, makes it difficult to discern the pattern of movement in RTM LMPs during the four earlier test-case days D1-D4. Fig. 15 therefore separately displays the RTM LMPs for test-case days D1-D4. The pattern of movement in the RTM LMPs depicted in Fig. 15 for D1-D4 is generally similar to the pattern of movement in the DAM LMPs depicted in Fig. 13a for D1-D4. However, moderate RTM LMP spiking is observed for hours 73 and 79.

The reason why spiking is observed in the RTM LMPs but not in the DAM LMPs can be better understood by considering the correlation between RTM/DAM price differences and net load forecast errors. Fig. 16 depicts the correlation for test-case days D1-D5 between: (i) the price difference [RTM LMP - DAM LMP]; and (ii) the net load forecast error as a percentage of



(a) Price difference (RTM LMP - DAM LMP)



(b)  $\widehat{NL}\%$ : Net load forecast error as a % of realized net load

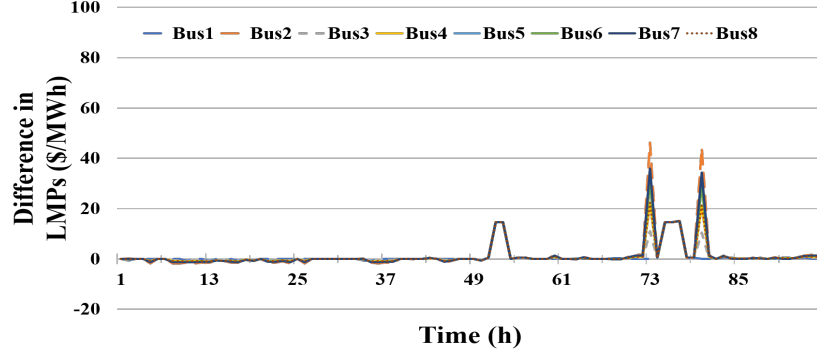
Figure 16: Correlation between price difference and net load forecast error for test-case days D1-D5

realized net load, calculated for each test-case hour  $H$  as

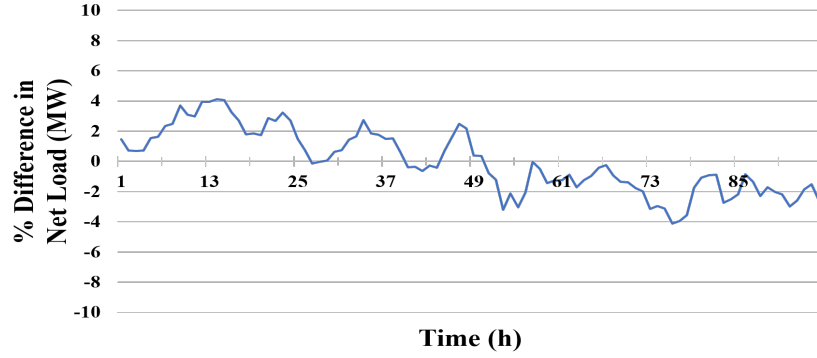
$$\widehat{NL}\% = \frac{\text{Day-Ahead Forecasted NL} - \text{Realized NL}}{\text{Realized NL}}. \quad (6)$$

Once again, the dramatic spike in the RTM LMP seen in Fig. 16 for hour 118 (i.e., the 22nd hour of the final test-case day D5) obscures correlation details for earlier hours. To better display these earlier correlations, Fig. 17 reports the correlations for test-case days D1-D4, omitting results for the final test-day D5.

Figs. 16 and 17 reveal the following general relationship: for each bus  $b$  and hour  $H$ , the RTM LMP is greater than the DAM LMP if and only if  $\widehat{NL}\%$



(a) Price difference (RTM LMP - DAM LMP)



(b)  $\widehat{NL}\%$ : Net load forecast error as a % of realized net load

Figure 17: Correlation between price difference and net load forecast error for test-case days D1-D4

is less than 0. Moreover, in some cases the RTM LMP significantly exceeds the DAM LMP. This results because, although sufficient capacity has been committed in the DAM to meet DAM-forecasted net load with 10% down/up reserve, the RTM forecasted net load (equated with realized net load in the test case) exceeds the DAM-forecasted net load to such an extent that the ISO is forced in the RTM to resort to the dispatch of peaker generation with relatively high marginal cost. For example, this is the explanation for the high RTM LMPs observed during hours 73, 80, 98 and 118.

Figs. 18 and 19 depict actual ERCOT RTM LMP contours captured from [42]. As can be seen, RTM LMPs can become very high at times, either in sub-regions or system wide. ERCOT is an “energy-only” wholesale power

market<sup>21</sup> that depends on high scarcity prices at times in order to permit generators to fully cover both their unit commitment (e.g., no-load) costs and their variable costs.

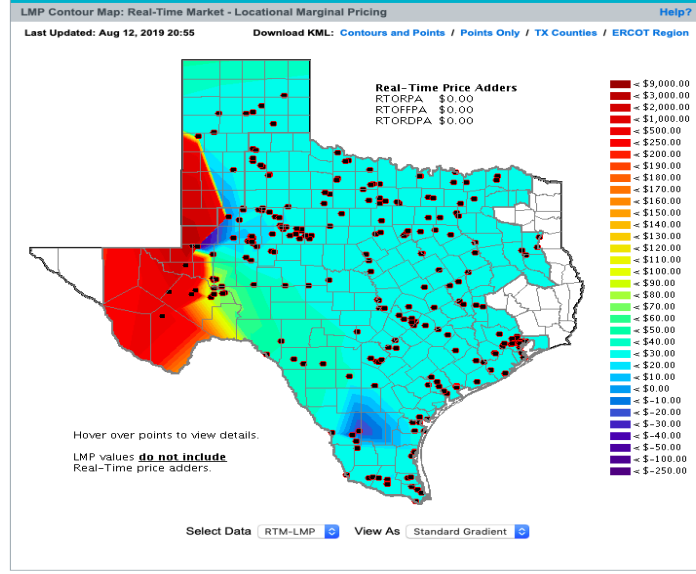


Figure 18: *Actual ERCOT RTM LMP Contour Map (August 12, 2019, 20:55) depicting a case in which RTM LMPs are strongly separated across the grid. Public Domain Source: [42]*

Finally, DAM and RTM dispatch schedules for the thirteen dispatchable generators G1-G13 are reported in Figs. 20 and 21 for test-case days D1-D5.

As seen in Fig. 20, in the DAM the ISO commits the relatively cheaper coal and nuclear generators (G2, G3, G5, G6, G8, G11 and G13) and schedules them at their maximum power capacities for much of the time. However, a dip in coal generator output occurs during hours 52-53 and 75-77. Specifically, dips in the generation of G2 and G5 are observed during hours 52-53; and dips in the generation of G2, G5, G11 and G13 are observed during hours 75-77. These dips occur because net load is relatively low during these hours, and the marginal generators that set the LMP for these hours are the

<sup>21</sup>An *energy-only wholesale power market* is a wholesale power market that does not include a separate capacity market for the encouragement of new investment in generation capacity.

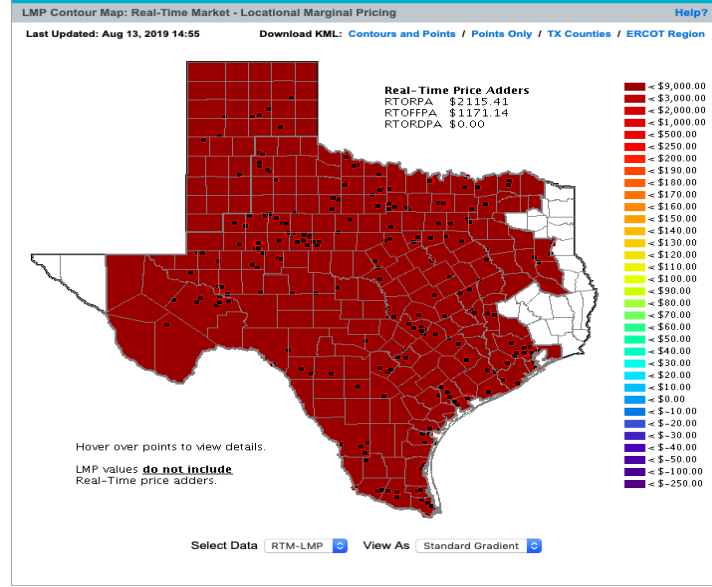


Figure 19: *Actual ERCOT RTM LMP Contour Map (August 13, 2019, 14:55) depicting a case in which all RTM LMPs are relatively high. Public Domain Source: [42]*

coal generators G2, G5, and G11. It is also interesting to note that these are the only hours during which there is no transmission congestion.

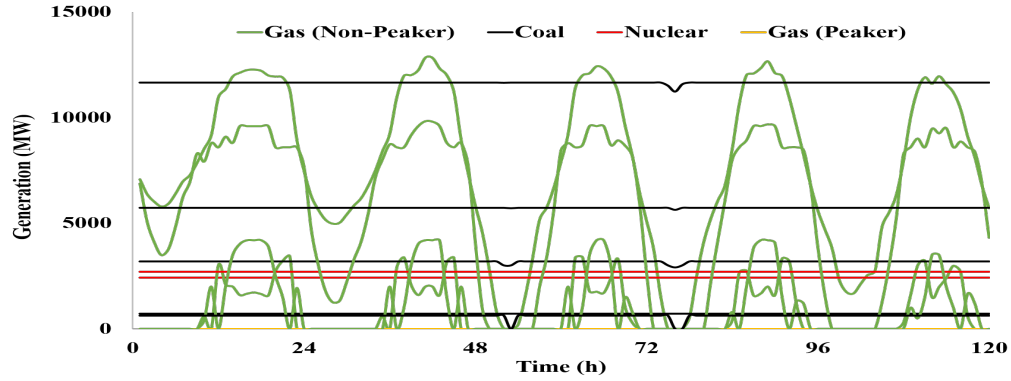


Figure 20: *DAM dispatch schedule for test-case days D1-D5*

In addition, in the DAM the ISO commits the non-peaker natural gas generators G1, G4, G10, and G12 and schedules their dispatch in merit order



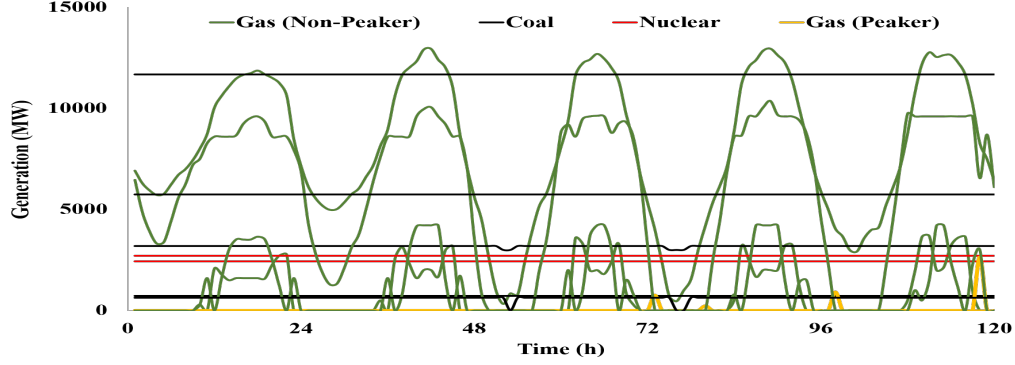


Figure 21: *RTM dispatch schedule for test-case days D1-D5*

(i.e., in the order of their marginal cost of generation), subject to transmission line congestion. The ISO also commits the two peaker generators G7 and G9 but schedules them at 0MW for each hour; that is, in the DAM the ISO treats G7 and G9 purely as reserve generation units.

However, as seen in Fig. 21, in the RTM the ISO dispatches the peaker generator G9 at positive power levels due to a changed net load forecast and changed congestion conditions. As previously explained at length, this results in relatively high RTM LMPs for hours 73, 80, 98 and 118. Note that the highest RTM LMP occurs at hour 118, when the scheduled dispatch of the peaker generator G9 is at its highest.

## 9. Test System Support for T & D Studies

### 9.1. Overview

AMES V5.0 [18, 19] has been integrated with PNNL’s *Framework for Network Co-Simulation (FNCS)* [1] in order to enable co-simulation of AMES with distribution system implementations for *Integrated Transmission and Distribution (ITD)* studies. Previous work [2, 3, 43, 44] indicates how this capability can be exploited for *Transactive Energy System (TES)* design research. This section briefly highlights further ongoing work along these lines at both ISU and PNNL.

### 9.2. Integration with the ISU ITD TES Platform

At ISU, AMES V5.0 and GridLAB-D [45] have been integrated by means of FNCS [1] into a framework referred to as the ITD TES Platform [2, 44].

An extended version of this platform (V2.0) is currently being used at ISU to study the operations of an *Independent Distribution System Operator (IDSO)* as a linking agent between a distribution system and a transmission system. Relatively small-scale ERCOT test cases with 8-bus transmission grids are being used to implement the transmission components for this ITD TES design work.

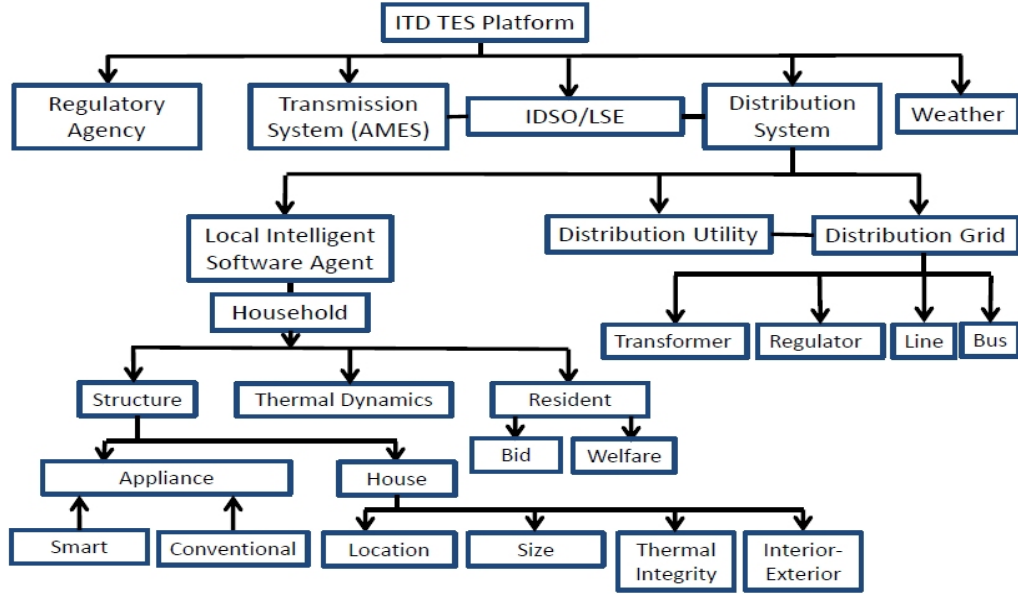


Figure 22: *Partial agent hierarchy for an ongoing ISU TES design study implemented by the ITD TES Platform (V2.0)*

For example, Fig. 22 depicts a partial agent hierarchy for an ongoing study focusing on the ITD performance of an IDSO-managed bid-based TES design. The IDSO manages a collection of households, each with a smart price-responsive HVAC system and a mixture of conventional appliances. The IDSO functions in the distribution system as an aggregator of household power-usage bids and ancillary service offers. The IDSO functions in the transmission system as a power procurer and as a provider of household-harnessed ancillary services (down/up power).

Fig. 23 depicts the key software components for this application, implemented by the ITD TES Platform (V2.0). Transmission and distribution aspects of the application are implemented by means of the AMES V5.0 and GridLAB-D components of this platform. FNCS is used to integrate AMES

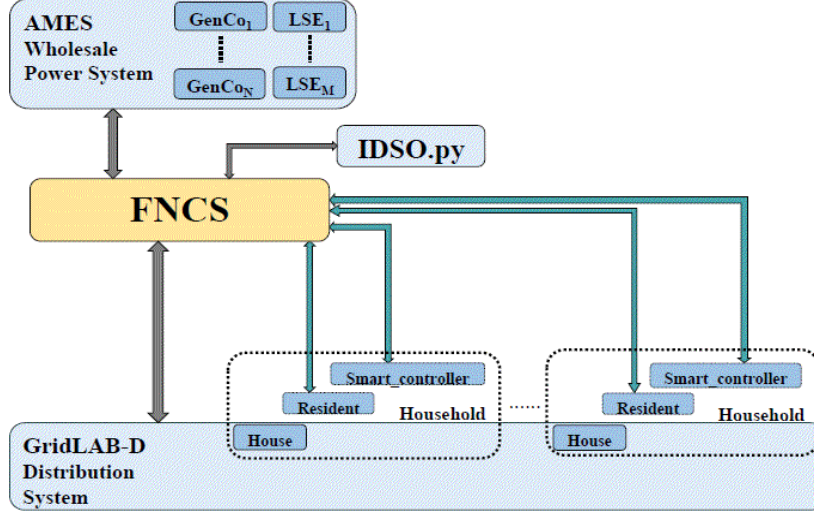


Figure 23: *Principal software components for an ongoing TES design study implemented by the ITD TES Platform (V2.0)*

V5.0 with GridLAB-D. FNCS also handles communication links among additional entities implemented in Python, such as the IDSO and the controllers for smart (price-responsive) household appliances.

### 9.3. Integration with the PNNL TESP

PNNL has developed a *Transactive Energy Simulation Platform (TESP)* to perform exploratory research into new market and control mechanisms for the grid [3]. Eight-bus and 200-bus versions of the ERCOT Test System described in the current paper are being used in a regional-scale study of transactive systems set in ERCOT’s footprint. These test cases are available at a GitHub repository; see [48].

As seen in Fig. 24, a code module called `fncsTSO.py` (for FNCS-based Transmission System Operator) manages the ERCOT model data, which is stored in a format similar to that used in MATPOWER [9] and PYPOWER [46]. PYPOWER is used to perform AC power flow solutions for the impact on substation bus voltage magnitudes. Because TESP is re-distributable [47], PYPOWER is used instead of the more full-featured MATPOWER for easier installation. AMES V5.0 [19] is used to perform SCUC and SCED calculations, as described in earlier sections of this study. At the appropriate times, `fncsTSO.py` will:

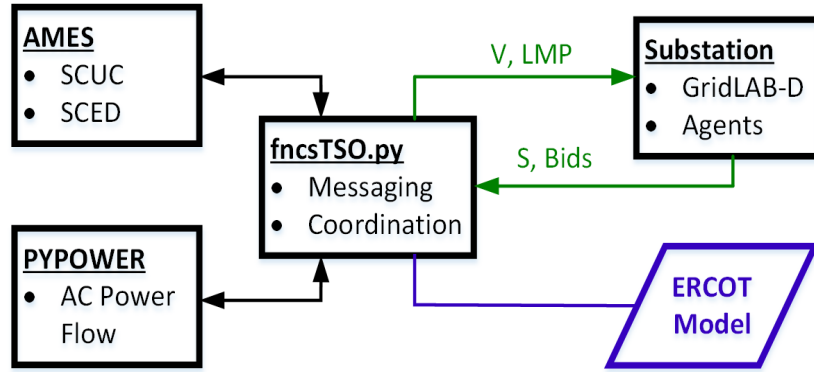


Figure 24: PNNL’s integration of the ERCOT Test System with AMES V5.0, PYPOWER, GridLAB-D, and other components of TESP

- Invoke AMES V5.0 to solve SCUC and SCED, including contingencies that are defined in the ERCOT model.
- Invoke PYPOWER to solve for bus voltages, including bulk generation schedules and swing bus designations based on the AMES results.
- Communicate with Distribution System Operators (DSOs) through one or more substations, which include both GridLAB-D simulations and transactive agents.

Typical values of the time step between these calculations are 5s for the substation and PYPOWER federates, 5min to 15min for the real-time market solution in AMES V5.0, and 24h for the day-ahead market solution in AMES V5.0. Fig. 24 highlights message traffic over FNCS between fncsTSO.py and the substation federate, which typically occurs every 5s. The message payloads include:

- The bus voltage magnitude,  $V$ , which affects the response of simulated loads in GridLAB-D.
- The locational marginal price (LMP), which only changes at each market clearing time step, i.e., a minimum 5min.
- The apparent power,  $S$ , including the actual real and reactive power, which will differ from the amounts bid. This will cause changes in transmission line flows, bus voltages and swing bus generation in PYPOWER.

- The bids, which include both price-responsive and fixed (non-price-responsive) components.

Each substation submits an aggregated bid from the many hundreds of participating devices connected to substation feeders. These aggregated bids are currently quadratic polynomials, but piecewise linear bids are also under consideration.

The price-responsive component of a bid can include aggregated generation and storage on the distribution system, and also price-responsive loads, e.g., smart thermostats and smart water heaters. PNNL’s study intends to quantify the impacts and benefits of price-sensitive load or demand bids in ISO/RTO-managed wholesale power markets such as ERCOT.

The fixed (non-price-responsive) component of a bid is estimated by the substation as the gross demand value (or forecast) minus the price-responsive load value (or forecast). The qualifier “fixed” refers only to lack of price dependency, not to lack of time variation. GridLAB-D simulates weather-dependent and occupant-dependent load effects, even for fixed load. These variations have to be balanced by reserves and the swing bus generation. Whenever the LMP changes, each substation agent will add its “markup” and then clear a local market of the participating devices, which then dispatch their local price-responsive resources. Aggregated bids have to be submitted before a market closing time, then the TSO market clears, then LMP messages go to the substations, and finally the substations clear their local device markets. See [47] for more detailed sequence diagrams.

PNNL’s version of an 8-bus ERCOT test case has one substation per DSO, which is enough to provide a test bed for agent software development. However, in order to properly capture regional diversity, PNNL has also developed a 200-bus ERCOT test case with multiple substations per DSO. The PNNL 200-bus ERCOT test case includes 120 generators, 47 extra-high-voltage (EHV) buses at 345 kV and 200 high-voltage (HV) buses at 138 kV. Each substation has its own weather data and a mixture of typical distribution feeders appropriate to the local area, e.g., urban, rural, suburban, and industrial; see [48].

The lower power capacity level  $P_g^{\min}$  for each dispatchable generator  $g$  is set as a percentage of  $g$ ’s upper power capacity level  $P_g^{\max}$  in accordance with  $g$ ’s fuel type. For nuclear,  $P^{\min}$  is set to 90% of  $P^{\max}$ ; and, for coal,  $P^{\min}$  is set to 50% of  $P^{\max}$ . For other fuel types, i.e., gas, wind and solar,  $P^{\min}$  is set to 10% of  $P^{\max}$ . The simulation time step ranges from 5s (regular power flow) to

15min (optimal power flow), so we applied a stochastic model of wind plant variability based on [49]. The stochastic parameters depend on wind plant size, and they reproduce plausible capacity factors and autocorrelations for each wind plant.

The following heuristics were used to build out the synthetic transmission grid for the PNNL 200-bus ERCOT test case:

- All loads are served from the HV buses, i.e., none from EHV. All generators at a clustered location are connected to the EHV bus if present, or the HV bus otherwise.
- An EHV bus was created at each clustered location that had a difference of 500 MW or more between local generation and local load.
- The EHV and HV networks were initially built out from Delaunay Triangulation, as described in Section 5.3.
- Based on results from PYPOWER, we pruned lines, added parallel lines, incremented transformer sizes, and added shunt compensation to eliminate overloads and voltage violations at peak load.

The resulting grid, depicted in Fig. 25, has 1.34 EHV lines per EHV bus, and 1.36 HV lines per HV bus.

Table 6: Positive sequence line parameters per circuit for the PNNL 200-bus ERCOT test case

Voltage kV	R1	X1	B1	Ratings	
	$\Omega/\text{mi}$	$\Omega/\text{mi}$	MVAR/mi	Amps	MVA
HV (138)	0.233	0.789	0.1039	655	157
EHV (345)	0.070	0.593	0.8616	1814	1084

Table 6 shows the typical positive sequence data used for EHV and HV lines, based on typical conductors and spacings at both voltage levels. In addition, transformer impedances of  $0.01 + j0.10$  pu were used, based on the transformer ratings between the EHV and HV buses at shared locations. Each transformer in the PNNL 200-bus ERCOT test case needed a tap ratio of 1.05 to maintain proper voltage on the HV system.

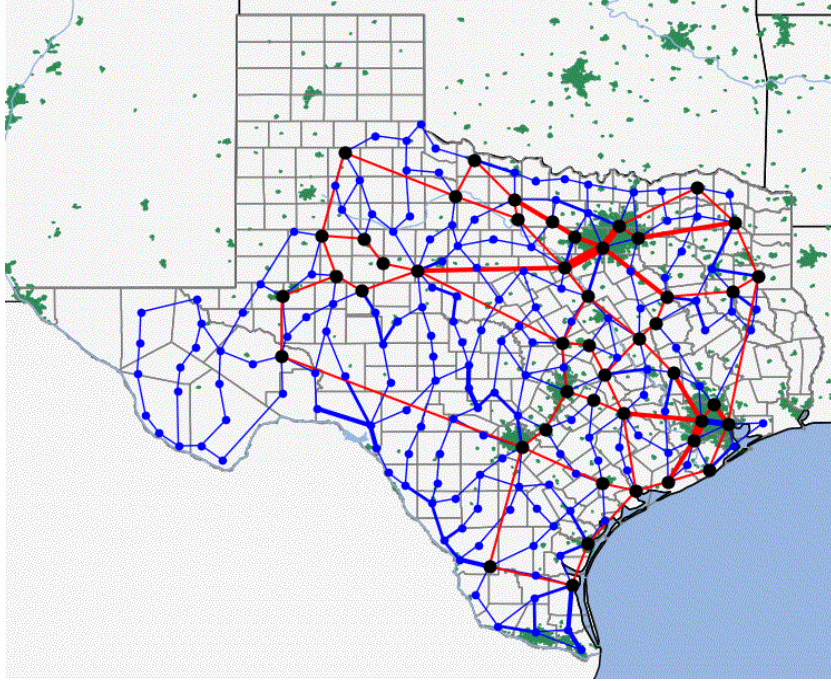


Figure 25: *Synthetic transmission grid for the PNNL 200-bus ERCOT test case, with 345-kV (red) and 138-kV (blue) transmission lines, superimposed on a background of county boundaries and urban areas (green)*

## 10. Conclusion

The ERCOT Test System developed and illustrated in this study permits users to evaluate the performance of ERCOT day-ahead and real-time markets operating over a high voltage transmission grid during successive simulated days. In default mode, the test system's software library permits these operations to be studied in existing forms under a range of operating conditions as determined by user-set parameters. Moreover, users can easily extend these software classes to permit the exploration of proposed new market design features.

More generally, users can integrate the ERCOT Test System as a component of the high level architecture FNCS [1] by a simple flag setting, thus permitting the study of coupled system operations. For example, users can study coupled transmission and distribution system operations. In ongoing studies these test system capabilities are permitting researchers at ISU and



PNNL to study potential roles for distribution system operators as linking entities operating at the interface of transmission and distribution systems.

## Acknowledgements

The authors thank Rohit Reddy Takkala for important work on a preliminary version of the ERCOT Test System. We are also very grateful to Qiuhua Huang (PNNL) and Mitchell Pelton (PNNL) for useful advice regarding test system design, coding, and testing. Finally, we thank Ross Baldick and Hailong Hui for helpful pointers to ERCOT resource materials.

## References

- [1] Ciraci, S, Daily, J, Fuller, J, et al. (2014) FNCS: A framework for power system and communication networks co-simulation. *Proc. of the Symposium on Theory of Modeling & Simulation*, San Diego, CA, April.
- [2] Nguyen, HT, Battula, S, Takkala, RR, Wang, Z, Tesfatsion, L (2019). An integrated transmission and distribution test system for evaluation of transactive energy designs. *Applied Energy* 240, pp. 666-679.
- [3] Huang, Q, McDermott, T, Tang, Y, Makhmalbaf, A, Hammerstrom, D, Fisher, A, Marinovici, L, Hardy, T (2019) Simulation-based valuation of transactive energy systems, *IEEE Transactions on Power Systems* 34(5), September, pp. 4138-4147. doi: 10.1109/TPWRS.2018.2838111.
- [4] Battula, S, Tesfatsion, L, McDermott, TE (2019), ERCOT Test System: Code and Data Repository  
<https://github.com/ITDProject/ERCOTTestSystem/tree/ISU>
- [5] Power System Test Case Archive, University of Washington. [Online]. Available: <http://www.ee.washington.edu/research/pstca/>
- [6] Grigg, C, et al., The IEEE reliability test system-1996: A report prepared by the reliability test system task force of the application of probability methods subcommittee, *IEEE Transactions on Power Systems* 14(3), Aug., pp. 1010-1020.
- [7] Dam, QB, Meliopoulos, APS, Heydt, G, Bose, A (2010) A breaker-oriented, three-phase IEEE 24-substation test system, *IEEE Transactions on Power Systems* 25(1), Feb., pp. 59-67.



- [8] Singh, AK, Pal, BC (2013) Report on the 68-bus 16-machine 5-area system, version 3.3, IEEE PES Task Force on Benchmark Systems for Stability Controls, Tech. Rep., December.
- [9] Zimmerman, R, Murillo-Snchez, C, Thomas, R (2011) MATPOWER: Steady-state operations, planning and analysis tools for power systems research and education, *IEEE Transactions on Power Systems* 26(1), February, pp. 12-19.
- [10] Lally, J (2002) Financial transmission rights: Auction example, ISO New England M-06, Technical Report, January.
- [11] Sun, J, Tesfatsion, L (2007) Dynamic testing of wholesale power market designs: An open-source agent-based framework. *Computational Economics* 30(3), pp. 291-327.
- [12] Li, H, Tesfatsion, L (2009) Development of open source software for power market research: The AMES test bed, *Journal of Energy Markets* 2(2), 111-128.
- [13] AMES (2020) The AMES Wholesale Power Market Test Bed: Homepage <http://www2.econ.iastate.edu/tesfatsi/AMESMarketHome.htm>
- [14] Li, F, Bo, R (2010) Small test systems for power system economic studies, in Power and Energy Society Gen. Meeting, IEEE, July, pp. 1-4.
- [15] FERC (2012) RTO unit commitment test system, Federal Energy Regulatory Commission, Technical Report, July.
- [16] Price, J, Goodin, J (2011) Reduced network modeling of WECC as a market design prototype, *Proceedings*, IEEE Power and Energy Society General Meeting, July.
- [17] Krishnamurthy, D, Li, W, Tesfatsion, L (2016) An 8-zone test system based on ISO New England data: Development and application. *IEEE Transactions on Power Systems* 31(1), pp. 234-246.
- [18] Tesfatsion, L, Battula, S (2019) Analytical SCUC/SCED Optimization Formulation for AMES V5.0, Working Paper, ISU Economics Department. <http://www2.econ.iastate.edu/tesfatsi/AnalyticalSCUCSCED0tForm.AMESPlatform.pdf>

- [19] Battula, S, Tesfatsion, L (2019), AMES V5.0 GitHub Repository <https://github.com/ITDProject/ERCOTTestSystem/tree/ISU/AMES-V5.0>
- [20] Gegner, KM, Birchfield, AB, Xu, T, Shetye, KS, Overbye, TJ (2016) A methodology for the creation of geographically realistic synthetic power flow models, *2016 IEEE Power and Energy Conference at Illinois (PECI)*, Urbana, IL, pp. 1-6.
- [21] Phillips, D, Xu, T, Overbye, TJ (2017) Analysis of economic criteria in the creation of realistic synthetic power systems. In *PowerTech, 2017*, IEEE Manchester, pp. 1-5.
- [22] Birchfield, AB, Gegner, KM, Xu, T, Shetye, KS, Overbye, TJ (2017) Statistical considerations in the creation of realistic synthetic power grids for geomagnetic disturbance studies, *IEEE Transactions on Power Systems* 32(2), pp. 1502-1510.
- [23] Birchfield, AB, Xu, T, Gegner, KM, Shetye, KS, Overbye, TJ (2017) Grid structural characteristics as validation criteria for synthetic networks, *IEEE Transactions on Power Systems* 32(4), pp. 3258-3265.
- [24] Birchfield, AB, Xu, T, Shetye, KS, Overbye, TJ (2018) Building synthetic power transmission networks of many voltage levels, spanning multiple areas, *51st Hawaii International Conf. on System Sciences*.
- [25] Xu, T, Birchfield, AB, Gegner, KM, Shetye, KS, Overbye, TJ (2017) Application of large-scale synthetic power system models for energy economic studies, *50th Hawaii International Conf. on System Sciences*.
- [26] Repository (2019) Repository of Synthetic Test Cases, Texas A&M University. <https://electricgrids.engr.tamu.edu/electric-grid-test-cases/activsg2000/>
- [27] ERCOT (2017) *ERCOT Nodal 101*, Electric Reliability Council of Texas, Course Modules 1-6.
- [28] ERCOT (2018) *Market Information*. Electric Reliability Council of Texas. <http://www.ercot.com/mktinfo>
- [29] ERCOT (2019a) *Nodal Protocols. Section 4: Day-Ahead Operations*, Electric Reliability Council of Texas, May 1.

- [30] ERCOT (2019b) *Nodal Protocols - Section 6: Adjustment Period and Real-time Operations*. Electric Reliability Council of Texas, January 1.
- [31] Baldick, R (2006) *Applied Optimization: Formulation and Algorithms for Engineering Systems*. Cambridge University Press, Cambridge, UK.
- [32] Liu, H., Tesfatsion, L., Chowdhury, A.A. (2009) Derivation of locational marginal prices for restructured wholesale power markets. *Journal of Energy Markets* 2(1), pp. 3-27.
- [33] Shiro, D, White, M (2015) Real-time price formation: Energy market offer design. *Tech. Session #11*. ISO-NE, Sturbridge, MA, June 19th.
- [34] Johnson, SC (1967) Hierarchical clustering schemes. *Psychometrika* 32(3), pp. 241-254.
- [35] Gärtner, B, Hoffmann, M (2013) *Computational Geometry Lecture Notes HS 2013*, Dept. of Computer Science, ETH, Zürich, Switzerland.
- [36] EIA (2019) *EIA-860 Data Site*, U.S. Energy Information Administration. <https://www.eia.gov/electricity/data/eia860/index.html>
- [37] ERCOT (2018b) Long-term hourly peak demand and energy forecast. *2019 ERCOT Planning*, Electric Reliability Council of Texas. December.
- [38] U.S. Census Bureau (2010) *U.S. Census Data*. <https://www2.census.gov/geo/docs/maps-data/data/gazetteer/>
- [39] ISONE (2019) *ISO New England Energy Offer Data*. [Online]. <http://www.iso-ne.com/isoexpress/web/reports/pricing/-/tree/day-ahead-energy-offer-data>
- [40] ERCOT (2019) *ERCOT Non-Dispatchable Generation Data*. <http://www.ercot.com/gridinfo/generation>
- [41] ERCOT (2019) *ERCOT Load Data*. <http://www.ercot.com/gridinfo/load>
- [42] ERCOT (2019) *LMP contour Map: Real-Time Market - Locational Marginal Pricing*, Electric Reliability Council of Texas. <http://www.ercot.com/content/cdr/contours/rtmLmp.html>

- [43] Hansen, J, Edgar, T, Daily, J, Wu, D (2017) Evaluating transactive controls of integrated transmission and distribution systems using the framework for network co-simulation, in: *American Control Conference (ACC)*, IEEE, pp. 4010-4017.
- [44] Battula, S, Tesfatsion, L, Wang, Z (2019) A transactive energy approach to distribution system design: Household formulation, Working Paper No. 19010, Economics Working Paper Series, Iowa State University, Ames, IA. [https://lib.dr.iastate.edu/econ\\_workingpapers/75](https://lib.dr.iastate.edu/econ_workingpapers/75)
- [45] Chassin, DP, Fuller, JC, Djilali, N (2014) GridLAB-D: An Agent-Based Simulation Framework for Smart Grids, *Journal of Applied Mathematics*, Volume 2014: Article ID 492320. <https://www.hindawi.com/journals/jam/2014/492320/>
- [46] Lincoln, R (2017) *PYPOWER*. Available: <https://pypi.python.org/pypi/PYPOWER>
- [47] PNNL (2017) *Transactive Energy Simulation Platform (TESP)*. Available: <https://tesp.readthedocs.io/en/latest/>
- [48] Schneider, KP, Chen, Y, Engle, D, Chassin, D (2009) A taxonomy of North American radial distribution feeders. *Proceedings, IEEE Power & Energy Society General Meeting*, pp. 1-6.
- [49] Chen, P, Pedersen, T, Bak-Jensen, B, Chen, Z (2010) ARIMA-based time series model of stochastic wind power generation, *IEEE Transactions on Power Systems* 25(2), pp. 667-676. doi:10.1109/TPWRS.2009.2033277.

## Appendix A: Software Installation

### A.1 Java Requirements

- AMES V5.0 [19] is based on Java, which can be downloaded from <https://java.com/en/download/>.
- The ANT tool is used to compile AMES V5.0.

### A.2 Python Requirements

AMES V5.0 uses the *Power System Simulation Toolbox (PSST)*, based on Python; thus, Python must be installed from the command line as follows:

```
cd C:/YourlocationtoAMES-v5.0/psst
pip install -e .
```

*Notes:* “pip install -e .” works to install PSST only if the PSST code has already been downloaded. The pip install command has a “period” at the end. PSST has its own dependencies, which are installed when the above command is passed.

### A.3 FNCS Requirement for Integration with PNNL TESP

- For integration with the PNNL TESP, AMES V5.0 requires the java libraries for FNCS to be located at C:/tesp/src/java or at some other designated location where the FNCS library is installed.
- Instructions from [https://tesp.readthedocs.io/en/stable/TESP\\_DesignDoc.html](https://tesp.readthedocs.io/en/stable/TESP_DesignDoc.html) are used to install the PNNL TESP, with FNCS installation as a pre-requisite.

## Appendix B: Key AMES V5.0 Classes

### AMES GUI (*AMESGUIFrame.java*)

- This class uses the *Graphical User Interface (GUI)* to load, create, and save a test case, to save output files, and to exert control over the overall simulation.
- This class was modified in AMES V4.0 (used in [17]) to permit inclusion of non-dispatchable generation (NDG) and storage units in test cases. AMES V5.0 retains this modification.
- If the ‘FNCSActive’ flag is set to ‘True’, ‘FNCS initialization’ and ‘FNCS end’ are called in this class. ‘FNCS initialization’ is called after the loading of an input test case to be simulated; and ‘FNCS end’ is called after output from the completed test-case simulation has been saved into a file.
- If the ‘FNCSActive’ flag is set to ‘False’, FNCS is not initialized for use in the simulation.

- *Note 1:* NDG and storage units must be explicitly specified in test cases; they cannot be added using the GUI.
- *Note 2:* The format of AMES test cases is .dat file.

#### *AMES Market (AMESMarket.java)*

- This is the main class for running test-case simulations, e.g., building market agents, constructing transmission grids, configuring parameter values, and so forth.
- The ‘buildSchedule’ method is used to create a schedule with a timer. ‘FNCS.time\_request’ is called inside this class, which is added to the schedule.
- The ISO operates the DAM and RTM at specific times, called by ‘iso.marketOperation(min, hour, day)’.

#### *Independent System Operator (ISO.java)*

- The ISO handles DAM and RTM operations during each day D.
- Each day D consists of 24 hours  $H = 1, \dots, 24$ .
- At the start of hour 10 on each day D, the ISO calls ‘PSSTDAMOpt’ to handle the day-D DAM SCUC/SCED optimization.
- At the beginning of each RTM, the ISO calls ‘PSSTRTMOpt’ (in turn ‘PSST SCED’) to handle the RTM SCED optimization.
- At the end of each day D, the optimal unit commitments for day D+1 determined in the day-D DAM SCUC/SCED optimization are stored for use as inputs in the RTM optimizations that the ISO conducts during day D+1.

#### *Generator Agent (GenAgent.java)*

- This class determines the attributes of a dispatchable generator using get and set methods.
- Each dispatchable generator submits a supply offer into the DAM on each day D that is then carried forward into the RTM operations held on day D+1.

- The dispatchable generator learning capabilities permitted by ‘GenAgent.java’ in earlier AMES versions are carried forward into ‘GenAgent.java’ for AMES V5.0, with no changes. This, each dispatchable generator  $g$  can be configured to learn over time how to submit strategic supply offers to increase its own net earnings.
- However, learning is currently turned off for each dispatchable generator  $g$  in AMES V5.0 by default settings  $M1_g=M2_g=M3_g=1$  for the learning parameters  $M1_g$ ,  $M2_g$ , and  $M3_g$  that controls the size of the feasible supply-offer set for generator  $g$ . Given these default settings, the feasible supply-offer set for  $g$  reduces to a single element: namely,  $g$ ’s true marginal cost curve.

#### *Load Serving Entity Agent (LSEAgent.java)*

- This class determines the attributes of a *Load Serving Entity (LSE)* using get and set methods.
- The LSE submits a demand bid into the DAM on each day  $D$  to service its customers’ power needs on day  $D+1$ .
- The LSE’s DAM demand bids can include both price-sensitive and fixed (non-price sensitive) components.

#### *Day-Ahead Market*

- At hour 6 on each day  $D$ , the ISO’s *Day-Ahead Market (DAM)* operation method is called to receive bids from generator and LSE agents.
- At hour 10 on each day  $D$ , the ‘DAMReferenceModel.dat’ file with the necessary parameters required for conducting the DAM SCUC/SCED optimization on day  $D$  is configured and is then used as the input file for performing the optimization.

#### *Real-Time Market*

- The default timing of each *Real-Time Market (RTM)* is in accordance with the timing depicted in Fig. 4.
- The time-line is partitioned into *Real-Time Operating Periods (RTOPs)*  $T$ , each with equal length  $RTOPDur$ .

- Each RTOP  $T$  is preceded by a real-time market  $\text{RTM}(T)$  with a look-ahead horizon  $\text{LAH}(T)$ . The purpose of  $\text{RTM}(T)$  is to ensure net-load balancing during  $T$ .

More precisely, let  $\text{DayDur} = 1440\text{min}$  denote the duration of each day  $D$ . The RTM timing is implemented as follows:

- The user sets  $\text{RTOPDur}$  (min) to a positive integer, subject to the admissibility condition that  $\text{RTOPDur}$  must be a divisor of  $\text{DayDur}$ .
- The number of RTOPs during each day  $D$  is then derived as  $\text{NRTOP} = \text{DayDur}/\text{RTOPDur}$ .
- One RTM with an associated LAH occurs prior to each RTOP to handle operations during RTOP.
- Every RTM has the same duration.
- Every LAH has the same duration.
- Let the RTOPs for any day  $D$  be denoted by  $(T_{D,1}, \dots, T_{D,K})$ , where  $K = \text{NRTOP}$ . Then  $\text{RTM} + \text{LAH}$  for any  $T_{D,k}$  with  $k > 1$  is configured to be held entirely within  $T_{D,k-1}$ , and  $\text{RTM} + \text{LAH}$  for  $T_{D,k}$  with  $k=1$  is configured to be held entirely within  $T_{D-1,K}$ .
- The number  $\text{NRTM}$  of daily RTMs is then equal to the number  $\text{NRTOP}$  of daily RTOPs.

Additional  $\text{RTM}(T)$  implementation aspects are as follows:

- LSEs serving only fixed (non-price-responsive) loads do not participate in  $\text{RTM}(T)$ . LSEs servicing dispatchable price-sensitive loads can bid this load into  $\text{RTM}(T)$ .<sup>22</sup>
- The ISO submits into  $\text{RTM}(T)$  a forecast for net fixed load (i.e., fixed load minus non-dispatchable generation) during period  $T$ .

---

<sup>22</sup>Recall from Section 3.3 that ERCOT permits QSEs to submit price-sensitive energy bids into the ERCOT RTM on behalf of LSEs that represent load resources whose power usage can be controlled by real-time telemetry.



- Similar to ‘DAMReferenceModel’, a reference file ‘RTMReferenceModel.dat’ is written in order to be given as an input file to the PSST RTM(T) optimization.
- Additionally, a file ‘RTUnitCommitments.dat’ containing the optimal DAM-determined unit commitments for T is given as an input file to the PSST RTM(T) optimization.
- AMES V5.0 treats these unit commitment values as exogenous inputs for the RTM(T) optimization. Consequently, the RTM(T) optimization reduces to a SCED optimization.

## Appendix C: Test System Nomenclature and User-Set Parameters

### C.1 Sets and Subsets

$\mathbb{B}$	Index set for the buses $b$ of a transmission grid;
$\mathbb{B}(z) \subseteq \mathbb{B}$	Subset of buses constituting reserve zone $z$ ;
$\mathbb{G}$	Index set for participant dispatchable generators $g$ ;
$\mathbb{G}(b) \subseteq \mathbb{G}$	Subset of dispatchable generators located at bus $b$ ;
$\mathbb{G}(z) \subseteq \mathbb{G}$	Subset of dispatchable generators located in reserve zone $z$ ;
$\mathbb{K}$	Index set for time-steps $k$ forming a partition of the operating period $T$ .
$\mathbb{L} \subseteq \mathbb{B} \times \mathbb{B}$	Index set for the lines $\ell$ of a transmission grid;
$\mathbb{L}_{O(b)} \subseteq \mathbb{L}$	Subset of transmission lines originating at bus $b$ ;
$\mathbb{L}_{E(b)} \subseteq \mathbb{L}$	Subset of transmission lines ending at bus $b$ ;
$\mathbb{LS}$	Index set for participant load-serving entities $j$ ;
$\mathbb{LS}(b) \subseteq \mathbb{LS}$	Subset of load-serving entities serving customers at bus $b$ ;
$\mathbb{LS}(z) \subseteq \mathbb{LS}$	Subset of load-serving entities serving customers in zone $z$ ;
$\mathbb{NG}$	Index set for participant non-dispatchable generators $n$ ;
$\mathbb{NG}(b) \subseteq \mathbb{NG}$	Subset of non-dispatchable generators located at bus $b$ ;
$\mathbb{NG}(z) \subseteq \mathbb{NG}$	Subset of non-dispatchable generators located in zone $z$ ;
$\mathbb{NS}_g(k)$	Index set for the segments $i$ used to form a piecewise-linear approximation for the total production cost function of $g$ ; at time-step $k$ ;
$\mathbb{Z}$	Set of indices $z = 1, \dots, NZ$ for reserve zones $\mathbb{B}(z)$ , which form a partition of $\mathbb{B}$ , i.e., $\cup_{z \in \mathbb{Z}} \mathbb{B}(z) = \mathbb{B}$ and $\mathbb{B}(z_i) \cap \mathbb{B}(z_j) = \emptyset$ for any $z_i$ and $z_j$ in $\mathbb{Z}$ with $i \neq j$ .

### C.2 User-Set Parameters

Tables 7-11 list the user-set parameters for AMES V5.0 [18, 19]. These parameters have to be properly configured in order to implement any specific ERCOT test case, such as the 8-Bus ERCOT DC Test Case. The user-set production cost coefficients in Table 8 are used by AMES V5.0 to construct an approximate total production cost function for each dispatchable generator  $g \in \mathbb{G}$ ; this construction is carefully explained in [18, Sec. 4]. A simulation run consists of simulated days 1,  $\dots$  MaxDay. If the value of  $\hat{v}_g(0)$  in Table 8 is positive (negative) for some dispatchable generator  $g \in \mathbb{G}$ , it indicates the number of consecutive hours prior to *and including* hour 0 that  $g$  has been turned on (off) where hour 0 is the hour immediately preceding the initial simulated day 1. Note that  $\hat{v}_g(0)$  cannot be zero, by definition.

Table 7: User-Set Parameters for the Grid

Parameter	Description
$DARRD \geq 0$	Day-ahead reserve requirement (decimal percent) for down-power system wide;
$DARRU \geq 0$	Day-ahead reserve requirement (decimal percent) for up-power system wide;
$DARRD(z) \geq 0$	Day-ahead reserve requirement (decimal percent) for down-power in reserve zone $z$ ;
$DARRU(z) \geq 0$	Day-ahead reserve requirement (decimal percent) for up-power in reserve zone $z$ ;
$E(\ell)$	End bus for transmission line $\ell$ ;
$F^{\max}(\ell) \geq 0$	Capacity limit (MW) for transmission line $\ell$ ;
$NB > 0$	Total number of transmission grid buses $b$ ;
$NZ > 0$	Total number of reserve zones $z$ ;
$O(\ell)$	Originating bus for transmission line $\ell$ ;
$RTRRD \geq 0$	Real-time reserve requirement (decimal percent) for down-power system wide;
$RTRRU \geq 0$	Real-time reserve requirement (decimal percent) for up-power system wide;
$RTRRD(z) \geq 0$	Real-time reserve requirement (decimal percent) for down-power in reserve zone $z$ ;
$RTRRU(z) \geq 0$	Real-time reserve requirement (decimal percent) for up-power in reserve zone $z$ ;
$S_o \geq 1$	Base apparent power (MW);
$V_o > 0$	Base voltage (line-to-line kV);
$X(\ell) > 0$	Reactance (ohms) for transmission line $\ell$ .

Table 8: User-Set Parameters for Dispatchable Generator Cost and Structural Attributes

Parameter	Description
$\text{atBus}_g$	The bus at which generator $g$ is located;
$a_g \geq 0$	Production cost function parameter (\$/hour) for $g$ ;
$b_g, c_g \geq 0$	Production cost function coefficients (\$/MWh, \$/[MW] <sup>2</sup> h) for $g$ ;
$CSC_g \geq 0$	Cold-start cost (\$) for $g$ ;
$CSH_g \geq 0$	Cold-start hours for $g$ ;
$DT_g \geq 0$	Minimum down-time (hours) for $g$ ;
$HSC_g \geq 0$	Hot-start cost (\$) for $g$ (must satisfy $HSC_g \leq CSC_g$ );
$\text{Money}_g^o > 0$	Initial money holdings (\$) for $g$ ;
$NRD_g$	Nominal ramp-down rate (MW/ $\Delta t$ ) for $g$ ;
$NRU_g$	Nominal ramp-up rate (MW/ $\Delta t$ ) for $g$ ;
$NSD_g$	Nominal shut-down rate (MW/ $\Delta t$ ) for $g$ ;
$NSU_g$	Nominal start-up rate (MW/ $\Delta t$ ) for $g$ ;
$NS_g \geq 1$	Number of segments used for the piecewise-linear approximation of $g$ 's total production cost function;
$p_g(0)$	Initial power output (MW) for $g$ ;
$P_g^{\max}$	Maximum power capacity (MW) for $g$ (must satisfy $P_g^{\max} \geq P_g^{\min}$ );
$P_g^{\min} \geq 0$	Minimum power capacity (MW) for a synchronized generator $g$ ;
$\text{SCost}_g \geq 0$	Sunk cost of $g$ ;
$SDC_g \geq 0$	Shut-down cost (\$) for $g$ ;
$UT_g \geq 0$	Minimum up-time (hours) for $g$ ;
$\hat{v}_g(0)$	Initial up-time/down-time status (number of hours) for $g$ .

Table 9: User-Set Parameters for Load and Non-Dispatchable Generation

Parameter	Description
$\text{atBus}_j$	The bus at which LSE $j$ is located;
$\text{atBus}_n$	The bus at which NDG $n$ is located;
$\hat{p}_j^{\text{DA}}(\text{H}) \geq 0$	LSE $j$ 's day-ahead forecast (MW) for the fixed load of its customers during hour H;
$\hat{p}_n^{\text{DA}}(\text{H}) \geq 0$	ISO's day-ahead forecast (MW) for the power output of NDG $n$ during hour H.

Table 10: User-Set Parameters for ISO Market Operations

Parameter	Description
$\text{RTOPDur} > 0$	Length (minutes) of a real-time operating period;
$\text{RTKDur} > 0$	Length (minutes) of each time-step of a real-time operating period;
$\Lambda^-, \Lambda^+ \geq 0$	Imbalance penalty weights (\$/MWh) for non-zero slack variables in the power balance constraints.

Table 11: User-Set Parameters for Simulation Control

Parameter	Description
$\text{FNCSActive}$	Flag indicating whether the simulation is to run with (1) or without (0) the use of FNCS;
$\text{MaxDay} \geq 1$	The maximum number (integer) of simulated days for each simulation run.

## Appendix D: 8-Bus ERCOT DC Test Case Inputs and Outputs

Table 12: 8-Bus ERCOT DC Test Case: Input configuration file for simulation-control parameters, transmission line attributes, and dispatchable generator attributes.

Base Values								
$S_0$	$V_0$							
100	345							
$\Lambda^-$	$\Lambda^+$	MaxDay	RTOPDur	RTKDur	FNCSActive			
1e6	1e6	6	60	5	True			
NB	NZ	DARRU	DARRD	RTRRU	RTRRD			
8	1	0.10	0.10	0.01	0.01			
Line								
From	To	$F^{max}$	$X$					
1	2	2168	61.156					
1	3	3252	41.867					
1	4	2168	78.240					
1	5	2168	58.096					
2	5	6504	14.625					
2	7	2168	61.718					
3	4	2168	43.617					
4	5	6504	24.636					
4	6	2168	59.374					
4	7	2168	63.445					
5	6	2168	42.079					
5	7	2168	49.331					
6	7	2168	59.050					
Gen ID	atBus	a	b	c	$P^{min}$	$P^{max}$	NS	Money <sup>o</sup>
1	1	2230	35	0.003	0	19978.8	10	10000
2	1	2128	19	0.0009	0	11114.8	10	10000
3	1	1250	8	0.00019	0	2430.0	10	10000
4	2	2230	56.5	0.0075	0	20711.7	10	10000
5	2	2128	19	0.0009	0	3190.3	10	10000
6	2	1250	8	0.00019	0	2708.6	10	10000
7	3	0	57.03	0.008	0	80.0	10	10000
8	3	2128	19	0.0009	0	720	10	10000
9	4	0	57.03	0.008	0	3438.2	10	10000
10	5	2230	45	0.006	0	10589.7	10	10000
11	5	2128	19	0.0009	0	5728.1	10	10000
12	7	2230	50	0.007	0	7385.0	10	10000
13	7	2128	19	0.0009	0	622.4	10	10000

Table 13: 8-Bus ERCOT DC Test Case: Forecasted net load (NL) profile used in DAM operations on the initial test-case day D0. Non-dispatchable generation is treated as negative load.

NL	Bus	H-1	H-2	H-3	H-04	H-5	H-6	H-7	H-8
1	1	17768.71	16701.24	16047.09	15647.84	15726.55	16139.0	16816.53	17224.51
2	2	13123.28	12337.5	11837.15	11534.56	11568.79	11814.18	12278.4	12562.73
3	3	-264.38	-253.29	-212.0	-191.9	-149.25	-46.83	9.4	23.31
4	4	-878.31	-844.18	-689.14	-614.4	-447.92	-46.3	177.98	259.91
5	5	8047.86	7565.97	7259.14	7073.57	7094.56	7245.04	7529.73	7688.39
6	6	295.36	277.46	267.6	261.41	264.1	274.41	287.78	278.41
7	7	2884.84	2704.57	2644.18	2599.89	2676.28	2900.8	3107.04	3220.28
8	8	30.19	28.38	27.23	26.54	26.62	27.18	28.25	27.67
NL	Bus	H-9	H-10	H-11	H-12	H-13	H-14	H-15	H-16
1	1	17988.93	18898.75	20036.25	21123.67	21962.52	22760.57	23257.19	23575.5
2	2	13085.4	13777.03	14605.99	15399.41	16018.08	16613.76	16993.77	17263.34
3	3	41.44	-118.41	-153.97	-150.77	-157.97	-194.71	-211.71	-283.29
4	4	440.45	68.3	25.28	43.36	14.4	-92.46	-186.44	-454.01
5	5	7942.41	8211.46	8664.8	9153.61	9538.19	9884.68	10138.32	10298.49
6	6	220.95	65.62	25.13	46.21	65.85	58.23	88.21	85.86
7	7	3463.6	3577.08	3797.88	3999.98	4137.9	4252.96	4295.99	4256.57
8	8	23.65	13.09	10.67	12.68	14.5	14.4	16.9	17.11
NL	Bus	H-17	H-18	H-19	H-20	H-21	H-22	H-23	H-24
1	1	23762.04	23610.39	23239.6	22419.94	21824.04	20992.47	19553.28	17915.6
2	2	17435.02	17305.47	17016.22	16405.6	15925.75	15312.31	14302.69	13147.66
3	3	-349.89	-308.12	-255.28	-137.19	19.64	39.39	-36.89	-112.41
4	4	-707.66	-562.64	-402.2	-161.01	278.99	329.7	21.05	-286.3
5	5	10401.44	10332.32	10181.8	9942.79	9754.22	9390.28	8771.13	8062.8
6	6	84.44	94.22	118.27	252.81	360.6	360.11	333.09	302.69
7	7	4196.92	4217.79	4195.42	4060.49	4057.09	3918.72	3543.27	3132.42
8	8	17.32	17.83	19.28	28.49	35.68	35.23	32.91	30.25

Table 14: 8-Bus ERCOT DC Test Case: LMPs (\$/MWh) by bus location and hour determined for day D1 in the day-D0 DAM

Bus	H-01	H-02	H-03	H-04	H-05	H-06	H-07	H-08
1	38.90	39.50	38.90	38.30	38.90	38.90	38.90	38.90
2	60.41	55.03	56.99	55.54	56.99	58.70	58.70	60.41
3	44.00	43.18	43.19	42.39	43.19	43.60	43.60	44.00
4	49.30	47.01	47.65	46.64	47.65	48.48	48.48	49.30
5	54.00	50.40	51.60	50.40	51.60	52.80	52.80	54.00
6	53.11	49.76	50.86	49.69	50.86	51.98	51.98	53.11
7	55.66	51.60	53.00	51.73	53.00	54.33	54.33	55.66
8	49.30	47.01	47.65	46.64	47.65	48.48	48.48	49.30
Bus	H-09	H-10	H-11	H-12	H-13	H-14	H-15	H-16
1	38.90	39.50	39.50	39.50	40.10	39.50	40.10	39.50
2	60.41	60.16	61.87	61.75	61.61	61.87	62.69	63.25
3	44.00	44.40	44.80	44.78	45.20	44.80	45.46	45.13
4	49.30	49.49	50.32	50.26	50.50	50.32	51.02	50.99
5	54.00	54.00	55.20	55.12	55.20	55.20	55.96	56.17
6	53.11	53.15	54.28	54.20	54.31	54.28	55.03	55.19
7	55.66	55.60	56.93	56.84	56.86	56.93	57.70	58.01
8	49.30	49.49	50.32	50.26	50.50	50.32	51.02	50.99
Bus	H-17	H-18	H-19	H-20	H-21	H-22	H-23	H-24
1	40.10	39.50	39.99	39.50	39.50	39.50	39.50	38.90
2	63.25	63.25	62.72	61.75	61.75	61.75	61.06	60.41
3	45.59	45.13	45.38	44.78	44.78	44.78	44.61	44.00
4	51.30	50.99	50.98	50.26	50.26	50.26	49.93	49.30
5	56.35	56.17	55.94	55.12	55.12	55.12	54.63	54.00
6	55.40	55.19	55.01	54.20	54.20	54.20	53.75	53.11
7	58.14	58.01	57.70	56.84	56.84	56.84	56.30	55.66
8	51.30	50.99	50.98	50.26	50.26	50.26	49.93	49.30